In Situ Measurements of Meteoric Ions

By JOSEPH M. GREBOWSKY[1] AND ARTHUR C. AIKIN[1]

[1]NASA Goddard Space Flight Center

1. Introduction

Extraterrestrial material is the source of metal ions in the Earth's atmosphere. Each year ~10^8 kg (Ceplecha, 1992) of material is intercepted by the Earth. The origin of this material is predominantly solar orbiting interplanetary debris from comets or asteroids that crosses the Earth's orbit. It contains a very small amount of interstellar material. On occasion the Earth passes through enhanced amounts of debris associated with the orbit of a decaying comet. This leads to enhanced meteor shower displays for up to several days. The number flux of shower material is typically several times the average sporadic background influx of material. Meteoric material is some of the earliest material formed in the solar system. By studying the relative elemental abundances of atmospheric metal ions, information can be gained on the chemical composition of cometary debris and the chemical makeup of the early solar system.

Using in situ sampling with rocket-borne ion mass spectrometers there have been approximately 50 flights that made measurements of the metal ion abundances at altitudes between 80 and 130 km. It is this altitude range where incoming meteoric particles are ablated, the larger ones giving rise to visible meteor displays. In several rocket measurements isotopic ratios of different atomic ion mass components and metal molecular ion concentrations have been determined and used to identify unambiguously the measured species and to investigate the processes controlling the metal ion distributions

The composition of the Earth's ionosphere was first sampled by an ion mass spectrometer flown on a rocket in 1956 (Johnson, et al., 1958). In 1958 a rocket-borne ion spectrometer identified, for the first time, a layer of metal ions (Istomin, 1963) near 95 km. These data were interpreted as evidence of an extraterrestrial rather than a terrestrial source. Istomin predicted: "It seems probable that with some improvement in the method that analysis of the ion composition in the E-region may be used for determining the chemical composition of those meteors which do not reach the ground. Particularly, we hope to get information about the composition difference between particles of different meteor showers and also sporadic and shower meteoroids". These visions categorized the aims of many subsequent rocket-borne ion mass spectrometer experiments in the lower ionosphere. Although the use such measurements to deduce the composition of different classes of meteoroids has not been successful, the past four decades of rocket observations have provided powerful sets of data for advancing our understanding of meteor ablation, meteoric composition, metal neutral and ion chemistry as well as ionospheric dynamics.

In addition to meteor ion populations measured in the lower ionosphere over the past 4 decades, metallic ions have also been detected from satellites hundreds of kilometers above the peak of visible meteor activity between 90 and 100 km. The first detection was by Hanson et al., 1970. This wasn't totally unanticipated because earlier ground based

observations of Ca^* resonantly scattered radiation in the twilight F-region revealed traces of Ca^+ up to 280 km (Broadfoot, 1967). Subsequent satellite ion composition measurements and resonant scattering observations explored these high altitude metal ion distributions to reveal a persistent global circulation of long-lived meteoric ions that move up from the meteoroid ablation region. The effect of this circulation on the lower altitude meteor layers has yet to be completely resolved, but it is evident that ion dynamics does play a significant role in the overall process by which infalling solar system particles leave their imprint on the ionosphere.

This chapter presents an overview of the in situ ion composition measurements of the metal ion distributions. It demonstrates how these observations have led to furthering our understanding of the interactions of meteoroids with the atmosphere and how the ablated material is processed to form persistent and complex metal ion layers.

2. Rocket Measurements Of Meteoric Ions

2.1 Early History and Instruments

The first rocket-borne ion mass spectrometer measurements of metal ions (Istomin, 1963) were made at middle latitudes and employed Bennett R-F ion mass spectrometers (Bennett, 1950). This instrument is a time-of-flight device that uses a fixed accelerating electric potential at the entrance aperture. Each ion species entering is accelerated to a unique speed, depending upon its mass. Radio frequency (rf) electric potentials are applied to a series of internal grids and the frequency is swept. For a given frequency, the ion species whose entrance—accelerated velocity lets it move through the sequence of grids in phase-resonance with the rf cycle, is maximally accelerated and will have larger kinetic energy exiting the rf grid section than other ion species present. A positive retarding potential is applied to a grid in front of the ion collector to reject the non-resonant ions. For this instrument, cycling the rf through an entire mass scan cycle takes the order of a few seconds so that the spatial resolution obtainable on a fast moving rocket is somewhat coarse. As a result it is not well suited for measuring narrow layers, but it is a reliable instrument that has yielded important measurements, particularly from satellites.

For the rocket flight detailed by Istomin (1963) the temporal sampling allowed only 100 complete mass spectra to be obtained between 92 and 206 km, but five spectra detected the presence of mass 24 and 26 amu ions. These ions were identified as Mg^+ - the ratio of the two ion currents collected was consistent with solar system Mg isotopic abundances. The ambient ionospheric species, NO^+ and O_2^+, were detected on all mass scans and were the dominant ions. Because of the complex dynamics of ions in the vicinity of fast moving rockets in dense atmospheric regions, it is not a simple matter to convert the collected ion currents into absolute ion concentrations without an independent measurement. Ion spectrometers provide a measure of relative ion composition. A second instrument is flown, or ground-based measurements are taken, to measure the electron/ion density along the flight path. The sum of the collected ion currents of all species is normalized to this electron density. The concentrations of individual ion species are then determined (using laboratory calibration, and/or theoretical modeling, of the spectometer's response to ion mass) from its proportion of the sum of all currents. Istomin (1963) used a UHF dispersion interferometer experiment to measure the electron density and found that the largest Mg^+ ion density was $\sim 10^4$ cm^{-3}. Similar peak densities were observed on both the upleg and downleg trajectories near 103 and 105 km respectively, implying the presence of a persistent metal ion layer. In addition, Mg^+ was

detected in one mass spectrum scan near 120 km indicating the presence of multiple layers. The species Fe^+ was also seen detected near the Mg^+ maximum and one mass scan contained the signature of positive ions with mass 40, presumably Ca^+ (or MgO^+}. The ratio of the latter ion concentration relative to the measured Mg^+ was ~ 1/25, which is close to meteor composition for Ca^+/Mg^+. Describing 2 earlier rocket experiments Istomin (1963) reported Fe^+ also at estimated concentrations of 10^4 - 10^5 cm^{-3} between 101 and 105 km. Mass 28 ions were detected near a Fe^+ occurrence that suggested it was Si^+ and not N_2^+ ions, which are often present in the ambient ionosphere.

These early Bennett ion spectrometer measurements provided the first measure of permanent ionization layers resulting from meteoritic deposition. Understanding of the underlying processes has been refined over subsequent years by rocket measurements made with much better spatial resolution and sensitivity. Still Istomin (1963)discovered many features of the metal ion distributions and their source that were seen in all subsequent flights. In addition the large measured concentrations of Mg^+ and Fe^+, exceeding 10^4 cm^{-3}, indicated their importance as potentially dominant ions in the ionosphere. Istomin's measured high dayside metal ion concentrations provided the first direct evidence that at night, where ambient ionosphere molecular ion concentrations decay, the lower low altitude ionosphere layers could be dominated by the longer-lived metal ions.

Before beginning an in—depth review of current understanding of the meteor ion layers derived from in situ ion composition measurements, we will describe the next published sounding rocket experiment. This is done to provide background for the workhorse ion spectrometer instrument, the quadrupole, which has dominated sounding rocket measurements of metal ions up to the present day. Narcissi and Bailey (1965) reported on the first launch of an ion mass spectrometer with the quadrupole mass filter system. It measured positive and negative ions from below 85 km to ~115, overlapping some altitudes sampled by Istomin (1963). Ion mass selection in this instrument is created by a 4 parallel (quadrupole) rod configuration, with its central axis perpendicular to the plane of the entrance aperture. Each opposite pair of rods has an electric potential difference (the bias voltage) applied to produce hyperbolic potential surfaces. By applying a sinusoidal voltage between the rods only a narrow range of mass/charge ions will traverse the length of the analyzer, to encounter the collector, for a fixed bias voltage. Other ion species are unstable in the time varying field configuration and are accelerated horizontally out of the central region. The mass spectrum is scanned by varying the RF and dc voltages, while keeping the voltage ratio between the rf amplitude and dc field constant. In order to make measurements in the altitude regime below 90 km, where high ambient gas pressures lead to performance degrading collisions within the instrument, a high speed, high capacity vacuum pump is required and was used. This quadrupole experiment provided the first measure of the entire lower altitude ionospheric region where meteors are observed.

The Narcisi and Bailey (1965) measurements are shown in Figure 1. The high ambient molecular ion concentrations at the higher altitudes saturated the instrument, but the total ion density in this region was available from electrostatic probes onboard. This plot was the first complete picture offered of a metal ion layer - one in which the Mg^+ (24 amu) ion concentration peaked at ~94 km with densities higher than 10^4 cm^{-3}. Similar layers were also present in the altitude profiles of other metal ion species. Ions with masses 25, 26, 23, and 40 amu wew identified as 2 minor isotopes of Mg^+, Na^+ and either Ca^+ or MgO^+ respectively. The instrument only sampled from 1 to 46 amu, so the presence of Fe^+

could not be ascertained. The Mg^+ isotope relative abundances compared favorably with solar system Mg abundances, as in the Istomin observations. Above 105 km all metal ion concentrations increased with altitude until apogee at 112 km. The 18 and 17 amu ions were water contamination products from the flight. The peak of the main metal layer was below the altitude inferred by Istomin whose experiment did not sample this low altitude region.

These initial experiments at midlatitudes, near midday, confirmed the presence of permanent layers of metal ions in the lower ionosphere that are of extraterrestrial origin. They also showed that multiple layers are present. Subsequent flights homed in on details of the distributions and controlling factors, which we will now discuss.

2.2 Metal Ion Layer Average Morphology

The continuous global influx of the sporadic background of meteoroids might be expected to lead, through ablation, to a single contiguous global layer of neutral metal atoms. The metal atoms below 100 km become ionized predominantly by charge exchange (e.g., Swider, 1969) with ambient ionosphere species - most notably NO^+ and O_2^+ as well as by photoionization. A simple picture, ignoring structured ion dynamics and atmospheric waves, is that there would be a single global-wide layer of meteoric ions in the ablation region. Sounding rocket experiments, such as the example in Figure 1 and another example shown in Figure 2, consistently find a layer of metal ions between 90 and 100 km, where most meteors are seen. The major metal ions in this main layer are Mg^+ and Fe^+. However, secondary layers of metal ions also repeatably appear above 100 km. This is seen in Figure 2, which shows a narrow metal layer near 108 km with a peak density larger than that of the lower layer. Other examples are shown in Figure 3, which depicts two encounters of layers above 100 km. The extreme narrowness of these upper layers, at times ~1 km, a thickness much shorter than diffusion scales, and the presence of a layer above the major meteoroid ablation region are indications that the upper layers are formed by processes different from the lower layer.

Although the main meteor ionization layer below 100 km, composed predominantly of Fe^+ and Mg^+, is persistent, and its structure often appears similar, as d4picted in Figures 1, 2 and 3, its most distinctive property, as seen from sounding rocket measurements, is its variability from flight to flight. Figure 4 shows 2 examples that contrast with the earlier figures. It shows one flight that encountered no metal ion layer below 100 km and one which detected an irregular layer for the species Mg^+ and none for Fe^+.

To statistically investigate the metal ion distributions, Grebowsky et al. (1998) and Grebowsky and Pesnell (1999) computer scanned all published sounding rocket metal ion density—altitude profiles. Interpolating each at 1 km altitude increments they set up a data base that could be statistically analyzed. For this review we have added to the original data base measurements that were not in the original studies (i.e., Earle et al., 1999; and Goldberg and Blumle, 1970, and corrected one profile that was erroneously scaled. There were 46 published ion spectrometer concentration profiles. A few publications, which presented only raw collected ion currents, were not used. Figure 5 contains a plot of the total metal ion densities from the database. An order of magnitude spread is observed with an average (in 2 km bins) peak concentration between 90 and 95 km. This variability and the location of the average is also seen for individual metal species as seen on the right of Figure 5. The average altitude profiles of three species Fe^+, Mg^+ and Ca^+ were culled from all sounding rocket measurements for middle (30-60°) and

high (>60°) latitudes. As seen the heavy ion Fe^+ is typically the dominant metal species and all species peak in the same region.

A different perspective on the changes in the metal ion profiles from flight to flight is depicted in Figure 6. This is a plot of all the individual rocket flight 1 km interpolated profiles of Fe^+ concentrations. The plot is broken into a middle latitude and high latitude zone. This is done because metal ion production and loss processes depend upon the ionosphere and atmosphere. Hence it is likely that the metal layers in the polar regions characterized by long winter (summer) nights (days) and auroral energetic particle deposition will differ from the middle latitude behavior. The middle/high latitude zones have different atmosphere/ionosphere profiles than the equatorial region. Thus low latitude measurements might form another unique grouping. Unfortunately, there have been only four low latitude rocket flights. One of these measurements is plotted in Figure 4 and two others (in Figure 10) will be discussed later. At all latitudes the main metal ion layer maximum moved about in the region between 90 and 100 km and the layer shape changed from flight to flight.

It is not possible with the limited rocket statistics to correlate in the main layer peak structure with local time or latitude. The measurements took place over all seasons and many years, under widely ranging solar and magnetic activity conditions. Still there are trends that appear in the data. Using the altitudes of the main layer maximum concentrations read off of published rocket ion composition plots there is evidence for a decrease in the peak altitude from middle to high latitudes and a day to night trend in each zone. For all Fe^+ concentration maxima, the average height and standard deviation at middle latitudes (17 samples) is 95.0±2.5 km compared to 92.3±3.5 km at high latitudes (15 cases). This trend is also evident in the altitude averages depicted in Figure 4. Looking at middle latitude measurements alone, the average dayside altitude (12 samples) is 93.9±1.3 km compared to the nighttime (5 samples) 97.5±2.8 km. For high latitudes (4 cases) it is 89.9±4.2 km in the day and 93.1±3.0 km at night (11 cases). The same trends are seen for Mg^+ the total metal ion density when that parameter and not individual species concentrations were published. The geometrical average of the middle latitude peak densities is 2×10^3 cm^{-3}. At high latitudes it is 4.6×10^3 cm^{-3} and in both regions the average width of the peaks at their half point is ~5 km.

Another prominent feature seen in Figure 6 is secondary ionization layers at high altitudes in the middle latitude region. At high latitudes the high altitudes layers are not evident, but some double—layer structures do appear below 100 km. Double—layer structures have not been observed on any of the equatorial experiments. The middle latitude upper layers are more variable in time than the main meteor ionization peak.

In the lower ionosphere, atmospheric horizontal winds drag ions which are affected by the Earth's magnetic field (**B**) which provides a barrier to cross **B** motions. The winds can move the ions freely along inclined magnetic field lines producing a vertical ion motion, but only in low altitude regions with dense atmospheric pressure can the neutral winds drag ions (velocity v)across the magnetic field lines. In the latter case, the resulting $\mathbf{v}\times\mathbf{B}$ Lorentz force on the ions can also lead to vertical ion motions. Vertical shears in the winds in the correct sense can lead to convergent ion flows and compression of the ion concentrations forming thin layers at the convergent nodes in the vertical ion drift. The physics behind this process was devised by Whitehead (1961). At high, auroral region latitudes, electric fields produced in the lower ionosphere from the magnetosphere are

intensified. These can transport and change the distribution of metal ions. These transport wind/electric field mechanisms operate down to ~90 km, where collisions in the dense neutral atmosphere inhibit any magnetic/electric field associated effects on the ions. These mechanisms could play a prominent role in the latitudinal dependence of the metal ion profiles (indicated in Figure 6).

The contrasting variability of the upper altitude layers compared to the main metal ion peak can be seen in Figure 3, which depicts a set of measurements separated by only 48 minutes, just before and after sunset. During the initial flight narrow layers were traversed near and above 110 km with the heavier ion Fe^+ layering several km above Si^+ and Mg^+. Narcisi et al.(1971) noted that a layer of Si^+ ions near 110 km is a prevalent feature of the dayside ionosphere, having been detected on many rocket flights. On the second flight, the Si^+ layer shifted to a higher altitude. The most prominent upper Fe^+ layer was now below 110 km. Either the small metal ion layer, seen near this altitude on the previous flight, grew or the upper layer moved downward, or the metal ions were distributed horizontally in patches. The main meteor ion layer profile did not change dramatically, but its metal ion densities did drop between the two flights. Although there are at times spatial separations seen between separate ion species, this is more evident in the upper layers. In the main meteor layer and even in most of the prominent upper layers all metal species tend to peak in tandem. Hence the metal ion composition in very prominent layers may provide a valid basis for inferring the composition of the parent meteoroid bodies, as is to be discussed next.

2.3 Composition of Deposited Material

Several ion composition studies have considered in detail the measured relative abundances of metal ions in the lower ionosphere. Figure 2 (left) is one such example, that shows the altitude distribution of many metal ion species (measured during a β-Taurids shower). The relative abundances in this case varied with altitude. Any abundance analysis must take this altitude variation into account, either by confining the sample to a specific altitude feature or by using total column densities. Also, ion mass spectrometers have a mass dependent response that must be considerd. It is assumed that such corrections were taken into account in the published data.

Table 1 summarizes the relative abundances cited in the literature from different ion spectrometer flights. All measurements listed are normalized to the total concentration of magnesium ions. In addition to the elements listed in Table 1, Hermann et al [1978] identified the presence of vanadium and copper metal ions. For comparison purposes with the likely source, the relative abundances of chrondritic material is shown in the first column. Each of the other columns, labeled by author, is a list of results from publications that explicitly specified the ratio of measured ion abundances (either referring to concentrations in the peak of a layer or to the total vertical content) to chrondritic abundance ratios. There is approximate agreement in most cases with the chrondritic values. This indicates that the source particles on average have essentially the composition of the Sun and the early solar system. They are not of terrestrial or lunar origin, since the compositions of the Earth and Moon have been differentiated over time from formation values by a variety of processes. Meteoric material is undifferentiated. T

A general conclusion can be drawn that the meteoric material from which the ions are derived, on average, has chrondritic composition. However, it is not possible to use precisely the ion data to deduce meteoroid composition without considering sources of

error in the data, details of the physical processes associated with meteoric deposition, and the nature of the interaction of metallic neutral and ionic elements with atmospheric oxygen and water vapor. The metal ions are also subject to dynamical effects in the atmosphere including neutral wind drag in the presence of the terrestrial magnetic field and electric fields. Using data outside of prominent layers yields composition results which are less in agreement with chrondrites than when ion concentrations are employed from within a layer (Krankowsky et al., 1972). Either the metal ion composition within the layers is the result of immediate local seeding by ablation, or dynamics may be focusing ions into a layer from adjacent regions. In the latter case, the peak species concentrations are proxies of the net vertical content.

The relative composition has usually been determined from the maximum concentration region of one of the layers, either the main layer or a prominent one above 100 km. With the exception of Kopp (1997) all of the composition studies cited in Table 1 followed this approach. Kopp (1997) used the measured total column amount of each ion. In the latter study the composition was in extraordinary agreement with chrondritic abundances. With the exception of sodium, potassium and cobalt, Krankowsky et al. (1972) found measurements to be within 40% of chrondritic composition and within 30% of stony-meteorite values. These elements were also overabundant in other data sets, suggesting differential ablation rates for different metals. Some inferred elements such as calcium and scandium have measured relative abundances far in excess of cosmic or terrestrial values. This is possible evidence for the confusion of these species with other species with the same charge to mass ratio as the metal. For example, MgO^+ could be confused with Ca^+ and $SiOH^+$ with Sc^+.

Several metallic ion species have the same mass to charge ratio as oxides or hydroxides of other metal species or as ambient ionospheric species. Comparison of the measured concentrations of metal atom isotopic masses for a species can be used to resolve the ambiguity. Table 2 lists cosmic abundances for isotopes of metal species normalized to the total magnesium abundance. The table includes ion isotope measurements from Krankowsky et al. [1972] and from 3 separate rocket flights studied by Steinweg et al. [1992]. The former study normalized all isotopes to the total magnesium ion concentration while the latter used Fe^+ as the reference. With the exception of sodium in the Krankowsky et al. study, whose concentration was three times greater than the cosmic abundance, the relative concentrations are in approximate agreement with cosmic abundances. All the studies yielded reasonable agreement with solar system values for the metal ion isotope ratios, but the relative percentages of some of the observed metal species were a factor of ten below average solar system values.

Contrary to the dominance of Mg over Fe in chondrites, measurements reveal a typical overabundance of iron ions (as seen in Table 1) but there are exceptions. For example, in Figure 4 (right) Mg^+ is more dominant than Fe^+, whereas in all the other individual profiles presented in this chapter Fe^+ had the larger concentration in the main meteor ion layer. Extracting the Fe^+/Mg^+ ratio at the main meteor layer peak from all published sounding rocket profiles the average turned out to be 2.4, with individual values ranging from 0.05 to 4.2. Mg^+ had the greatest density for 21% of the cases. For shower measurements the average ratio was nearly the same, 2.2, with Fe^+ always dominant. There is an unexplained variability in Mg^+/Fe^+. Possible explanations suggested by McNeil et al. (2001) include variations in meteoroid composition or differential ablation. LIDAR observations (von Zahn et al., 1999) and modeling (McNeil et al., 1998) have

demonstrated the importance of differential ablation for species with different volatilities. For example the peak Na deposition due to ablation is modeled to lay more than 10 km above that of Mg. Hence the metal atom and associated ionospheric metal ion composition could change with altitude. However, the detailed rocket metal ion composition relations (Tables 1 and 2) do not indicate an altitude dependence. Neutral metal atoms are converted to ions by charge exchange with ambient O_2^+ and NO^+ and the chemistry is affected by species-dependent chemical interactions with the atmosphere. These processes, along with ionospheric dynamics, will blur the altitude imprint of differential ablation on the metal ions but still leave differences between the relative abundances of the measured metal ions compared to meteoroid atomic atom composition.

2.4 Chemistry of Metal Ions

The multiplicity of ion species, combined with limited ion spectrometer mass resolution, can contribute to an uncertainty in the assignment of mass to a particular metal ion isotope. The chemical processing of ablation products to ions is another error source. Table 3 provides a list of all observed ion masses that have been related to metal ion molecular species. Possible duplicate ion identifications are indicated. With the exception of Si^+, N_2^+, atomic metal ion species do not have the same mass as the major ionospheric ions O_2^+, NO^+, O^+, and N_2^+ or their isotopes, A notable exception is Si^+ that has the same ratio as N_2^+. The appearance of narrow 28 amu ion layers, particularly within or near layers of other metal ions can be taken as proof that Si^+ is the proper identification. An interesting case of ambiguity is the positive ion with mass 45 amu, which was first reported to be scandium by Goldberg and Aikin (1973, see Table 3. The difficulty with this assignment is that the observed abundance is 600 times the cosmic abundance of Sc^+. The same mass, with similar abundance, has been observed in other investigations (Zbinden et al, 1975). One explanation is that the species is $SiOH^+$, which forms in the reaction (Fahey et al. 1981)

$$Si^+ + H_2O \rightarrow SiOH^+ + H. \qquad (2.1)$$

$SiOH^+$ disappears rapidly by dissociative recombination with electrons so that a significant amount of water must be present at the altitude of the metal ion layer to insure a continued presence of $SiOH^+$. Zbinden et al (1975) attributed the water source to rocket outgassing.

Metal ions are converted to neutral metals either by radiative recombination with ambient electrons

$$X^+ + e \rightarrow X + h\nu \qquad (2.2)$$

Or, by conversion into a molecular ion (such as XO^+) followed by dissociative recombination with electrons

$$XO^+ + e \rightarrow X + O, \qquad (2.3)$$

$$XO_2^+ + e \rightarrow X + O_2. \qquad (2.4)$$

Radiative recombination (proceeds at a rate of about 1×10^{-12} cm^3 s^{-1} while dissociative recombination at 300°K is about 5×10^{-7} cm^3 s^{-1} for most molecular ions. Thus atomic

ions have a lifetime 5 orders of magnitude longer than molecular ions. For an electron density of 1×10^{5} cm^{-3}, a nominal dayside ionospheric density, the respective lifetimes of atomic and molecular ions are 10^{7} and 20 seconds. At high altitudes, above the ablation region, where transformation of atomic ions into molecular ions by interaction with atmospheric molecules is not significant, metal ions prevail only in atomic form. Molecular ion concentrations decay more rapidly as the electron density increases. This effect is the reason that the narrow (Sporadic E) ionosphere layers are often comprised of a high percentage of metal ions relative to the ambient ions NO^{+} and O_2^{+}.

At lower altitudes in the ablation region, and below, the atomic metal ions are chemically rapidly converted into molecular ions and rapidly disappear with decreasing altitude. Table 3 lists the variety of metal ion compounds that have been measured. Species range from simple oxides such as AlO^{+}, SiO^{+}, and FeO^{+} to more complex oxygenated species (e.g. $FeO2^{+}$). There are also hydrated constituents like $CaOH^{+}$ and $FeOH^{+}$. Further water can attach directly to form species such as $Fe^{+}(H_2O)$ and $Fe^{+}(H_2O)_2$. These molecules form typically in the cold summer mesopause region at high latitudes (Goldberg and Witt, 1977).

Laboratory studies (Plane, 1991) have shown that metals react with molecular oxygen to form oxides in the reaction

$$X^{+} + O_2 + M \rightarrow XO_2^{+} + M \qquad (2.5)$$

where X represents any metal such as Mg or Fe and M is a third body, which in the atmosphere is either O_2 or N_2. N_2 can be substituted for O_2 giving rise to XN_2 (Plane et al., 1999). Metal oxides can also be formed by

$$X^{+} + O + M \rightarrow XO^{+} + M, \qquad (2.6)$$

and

$$X^{+} + O_3 \rightarrow XO^{+} + O_2. \qquad (2.7)$$

Metal hydroxides can be formed by

$$X^{+} + H_2O_2 \rightarrow XOH^{+} + OH. \qquad (2.8)$$

The ion XO_2^{+} is produced by

$$XO^{+} + O_2 + M \rightarrow XO_2^{+} + M \qquad (2.9)$$

while

$$XO_2^{+} + O \rightarrow XO^{+} + O_2^{+} \qquad (2.10)$$

converts XO_2^{+} to XO^{+}. In the case of elements such as sodium and silicon, formation of metal hydroxyls occur by

$$XO^{+} + H_2O \rightarrow XOH^{+} + OH \qquad (2.11)$$

These processes account for the metal molecular ions measured in the ablation zone below 100 km.

Metal compounds are absent above ~100 km and become dominant over atomic metal ions below 85 km. Above 100 km atomic oxygen increases dramatically. In this environment

$$XO^{+} + O \rightarrow X^{+} + O_2 \qquad (2.12)$$

in addition to dissociative recombination reactions destroys XO^+ and XO_2^+. Below 85 km the atmosphere electron density is reduced, decreasing the effectiveness of dissociative recombination in destroying XO^+ and XO_2^+. Also below 85 km, O_3, O_2 and H_2O increase in concentration, leading to enhanced production of XO^+, XO_2^+ and XOH^+. The combination of increased production and decreased loss leads to increased metal oxide ion concentrations.

At low altitudes atmospheric aerosols lead to the disappearance of metal ions through the production of clustered metallic ion species (e.g., Kopp and Hermann, 1984) which rapidly become neutralized. Figure 7 shows a case where the bottom of the main meteor ion layer overlaps the upper boundary of the hydrated ion layer (the molecular ion with mass 37 amu corresponds to the cluster $H^+H_2O_2$). Some particularly sharp cutoffs in the metallic ion layers were measured at high latitudes above noctilucent clouds (Kopp et al., 1985) as seen in Figure 7. The origin of the decrease of ionization in the vicinity of noctilucent clouds is the attachment of free electrons and ions to cloud particles, increasing the loss rate of the metal ions.

2.5 Meteor Showers

One goal of sounding rocket ion composition experiments has been to infer the composition of the parent bodies of meteor showers. Model calculations by McNeil (2001), McNeil (1999) and Grebowsky and Pesnell (1999) detail how individual streams might affect the ionosphere. However measurements are needed to establish the extent of meteor shower effects. An increase in the number of individual ionization trails is associated with a shower, but this ionization quickly disperses and may not lead to a lasting enhancement of ion concentration in the ionosphere. However, during the event, additional ablated neutral atoms are added to the atmosphere. The subsequent ionization of this new material, by either photoionization or charge transfer processes with ambient ionosphere species, has the potential to produce measurable lasting ionospheric effects separable from the persistent layers produced by the sporadic background of meteoroids. It has been commonly assumed in previous publications that the metal ion distributions observed during a shower are due to the shower itself. As will be shown, the rocket evidence points in this direction, but statistics are still not sufficient, in terms of the number of experiments and the control of the conditions under which the measurements were made, to remove all ambiguity.

Figure 8 shows measurements taken during, or closely after 2 major showers. One of the samples is at middle latitudes and the other in a high latitude, auroral, energetic particle precipitation zone. The maximum Fe^+, Mg^+ metal concentrations for both events were near 10^4 cm^{-3}. Compared to the ensemble of all Fe^+ densities (Figure 5), they fall within the upper quartile of all observed concentrations below 100 km. More evidence for a shower effect is seen in Figure 7. The data on the right were obtained during a Perseids shower and the measurements on the left were obtained from the same location a few weeks earlier. The shower-period peak metal ion density was almost two orders of magnitude above that of the earlier period. As appealing as it is to conclude a shower effect is present from these individual measurements, there are still uncertainties. For example, the high latitude shower event in Figure 7 was characterized by significant enhancement of the NO^+ concentration compared to the non-shower period and the bottom of the pre-shower metal ion layer was apparently eroded by losses associated with aerosols. Hence background ambient conditions were very different between the two flights making a comparison for meteoric effects uncertain.

In an attempt to resolve this issue Grebowsky et al. (1998) compared published shower measurements of the total concentrations of metal ions to the ensemble of all published metal concentrations. The results are shown in Figure 9. For middle latitudes there were only 4 measurements near or immediately following showers. These shower profiles all had prominent high altitude layers with metal ion concentrations exceeding quiet time layer concentrations at the same altitudes. In the main metal ion layer region, 3 of the the shower events also showed enhanced metal ion densities compared to the non-shower data. However, the flight associated with the β-Taurids (Figure 4, left) didn't find a metal ion layer below 100 km (Figure 4, left). At high latitudes (Figure 9) the two shower—period profiles did not have the highest densities. Interestingly, all six shower flights showed double layer structures. The evidence points toward an enhancement of the metal ion layer concentrations during showers at middle latitudes. However the number of data samples is limited and the effects of the different ionospheric and atmospheric conditions under which the rocket measurements were made have not been investigated. The detailed ion composition studies, discussed earlier, did not show any significant differences between shower and non-shower periods. This point was made by Kopp (1997) and is verifiable by a comparison of the measurements in Tables 1 and 2, in which the Zbinden et al. (1975) and Golberg and Aikin (1973) measurements were for shower periods. Further studies are needed to definitively establish the impact of the showers on the ionospheric metal ion distributions.

2.6 Sources of Variability in Metal Ion Layers

It is a common assumption in the analyses of the physics of the meteor ion layer that the sporadic background of incoming particles is in an equilibrium state in which day to day variations in their
properties are not significant. Meteor shower events, on the other hand, introduce discrete time dependent bursts of different particle populations into the atmosphere. This can have an impact on the metal ion distributions. On the other hand, LIDAR, ground-based radio/radar soundings, and in situ ion composition studies have shown that secular and dynamic plasma and atmospheric processes have direct control of the lower ionosphere layers. These are sources for much of the observed structure in the metal ion distributions and they must be considered when looking for meteor shower effects in rocket—borne ion composition measurements.

Atmospheric/ionospheric dynamics are responsible for the complex narrow, time varying layers in the lower ionosphere, leading to complex "sporadic-E" structures in which metal ions are often the dominant ion. One clear example of the temporal impact of ionospheric dynamics on the main meteor ion layer is shown in Figure 10 (from Aikin and Goldberg, 1973). The metal layer, with Mg^+ dominant, dropped 7 km in the 4 1/2 hours between the two launches. The metal ion vertical content did not change, while the peak metal ion density increased and the concentration of ambient NO^+ decreased. The altitude decrease was in phase with the downward F region drift measured at the same time by an ionosonde, and the NO^+ density decrease was consistent with enhanced dissociative recombination due to the increasing electron density resulting from enhancements metal ion concentrations. Hence, the metal ion layer was compressed as it moved down.

Ionospheric electric fields and atmospheric waves not only move the meteor layers around, but they can have an ion spectrometer effect on the metal species as well. That

is, ion species can be separated in space. Examples of this are shown in Figure 11 – in both cases there is ~1 km separation between the Fe^+ and the lighter Mg^+ layers. This behavior was predicted by Chimonas (1969) as a characteristic for metal layers formed and transported downward in phase with the nodes of the horizontal wind. The neutral wind is more effective in dragging the lower mass ions. The presence of this process could at times compromise the use of local measurements of relative metal ion composition as indicators of meteoroid composition.

The effects of dynamics are predominant for the upper metal ion layers but also influence the main meteor ionization layer. The topside slope of the latter layer can vary on short time scales compared to the ablation/chemistry/diffusion processes that would produce the layer under quiescent conditions. On the other hand, the bottomside of the main metal ion layer near and below 90 km is not sensitive to externally driven ion dynamics. This side of the layer is dominated by local ion-neutral chemistry as detailed in section 2.4. The location of the lower boundary of the metal ion layer varies from flight-to-flight (see Figure 6), but the bottomside altitude contours contain no prominent irregular structure – in contrast to the topside region. The chemistry is controlled by aerosols and oxygen profiles which change with season, time of day, and atmospheric/auroral activity (e.g., Kopp and Hermann, 1984; Arnold and Krankowsky, 1977; and Narcissi, 1973). Hence the bottom of the main layer has distinctly different sources of variability than the upper side. The combination of dynamics and variations in chemistry lead to complex metal ion layer behaviors.

3. Satellite In Situ Measurements Of Meteoric Ions

Sounding rockets at middle latitudes frequently traverse metal ion layers above 100 km, the result of long-lived atomic metal ions that are entrapped in convergent ion velocity nodes produced by atmospheric waves. Since the main metal ion production is at lower altitudes, upward transport is required, unless the descending layer nodes are directly seeded by the immediate ionization of meteoric debris at high altitudes. The latter could take place by impact ionization of very fast particles that, in addition to ablating at higher altitudes than slower particles, also have more energy available to produce ionization by impact ionization of the ablated gases. This high altitude seeding could be important for high-speed meteor showers, such as the Leonids and Perseids with average speeds of the order of 60-70 km/s (compared to the ~20 km/s average speeds of the sporadic meteoroids). If local production of metal ions in the convergent drift nodes is not significant, the metal ion layers above 100 km must consist of long-lived metal ionization that had been previously transported upwards from the ablation region, before being entrapped in narrow layers by atmospheric waves. Evidence for the importance of this upward transport has been found in satellite observations of metal ions at much higher altitudes than the sounding rocket observed layers.

The near-Earth detection of metal ion layers in the vicinity of ~100 km was not really surprising since this is the region where ionization is evident in meteors. Early ground-based observations provided evidence for the presence of meteoric ions at much higher altitudes. Resonantly backscattered solar radiation emissions from Ca^+ which were seen originating from altitudes as high as 280 km (Broadfoot, 1967). The first in situ measurements of metal ions from a satellite, (OGO-6), found Fe^+ concentrations exceeding 100 cm^{-3} near 500 km (Hanson and Sanatani, 1970). This discovery was made, not with an ion mass spectrometer, but by interpreting changes in the current collected on an ion trap experiment as a retarding potential was enhanced to eliminate the collection of low

mass ions. A follow-up study substantiated the presence of Fe^+ and found traces at altitudes as high as 1000 km (Hanson et al., 1972). These initial Fe^+ high altitude detections were at low latitudes and were attributed to electrodynamical lifting of the ions from the meteor ablation source region. A later study (Grebowsky and Brinton, 1978) discovered similar large concentrations of Fe^+ at altitudes of several hundred kilometers at middle and high latitudes.

Figure 12 shows a satellite measurement in which Fe^+ was found to be the dominant ion near 234 km. These data were taken from a satellite with a nearly circular orbit. A more descriptive example is shown in Figure 13, which uses data from 2 consecutive eccentric orbits of Atmosphere Explorer C. Fe^+ data were obtained with BIMS (Bennett Ion Mass Spectrometer) and Mg^+ data with MIMS (Magnetic Ion Mass Spectrometer). The latter instrument (Hoffman et al., 1973) used a magnetic field to separate ion masses by their differing gyroradii. BIMS (Brinton et al., 1973) had reduced sensitivity and different temporal resolution of the metal ions than did MIMS. The absence of Fe^+ when Mg^+ was present is an instrumental effect. Metal ions were encountered from the spacecraft's perigee altitude near 140 km to above 200 km with concentrations comparable to those of rocket measurements in the main meteor ion layer. The Mg^+ concentration tapers off as the ionospheric density (mostly O^+ ions) approaches its peak value in the F-Layer. There was a large change in the Mg^+ concentration at the lower altitude in the 2 hours between the orbits but the metals persisted continuously along the satellite track below 240 km.

Satellite ion composition measurements are much more comprehensive than sounding rocket measurements and provide statistically meaningful studies of the global, high altitude metal ion distributions. Kumar and Hanson (1980) provided the first global overview of their altitude distribution by studying several metal ion species from Atmosphere Explorer, Dynamics Explorer and OGO 6 spacecraft. The metal ions were encountered in all latitude zones, with the highest percentage of detection from 200 to above 300 km, corresponding to the typical bottom side of the F-layer. The metal ions were found at altitudes exceeding 300 in the equatorial region more often than at other latitudes.

The global distribution of the high altitude metal ions is depicted in Figure 14. This is a plot of the locations where Fe^+ ions were detected with concentrations exceeding 30 ions/cm^3, between 150 and 400 km, from Atmosphere Explorer C (with a high orbital inclination) and Atmosphere Explorer E (a near equatorial orbit). A strong dawn-dusk local time asymmetry in the low latitude occurrence frequencies is apparent with more patches traversed in the afternoon-dusk regions. This was first noted in the study of Kumar and Hanson (1980). At higher latitudes Fe^+ tends to be concentrated in a mid-latitude band at night between 50-60 degrees that extends through dawn. There is another separate intensified band on the dayside of the polar cap.

Mechanisms for transporting the long-lived metal ions from their source region below 100 km upward have been identified. The processes are depicted schematically in Figure 15. Low latitude metallic ions can be pulled upwards out of the main meteor layer region by either: 1. a vertical polarization electric field associated with the equatorial dynamo; or 2. the Lorenz force **Ueast**×**B** (**Ueast** is the eastward component of the neutral wind and **B** is the magnetic field vector). Once the ions move to a region where the ion collision frequency is less than the ion gyrofrequency, the neutral wind and electric field can no longer drive the ions across the magnetic field. However, the ions can still be driven

upwards across the field lines by the E×B convection due to the dynamo electric field. The metal ions eventually will fall to lower altitudes. The prevailing horizontal neutral wind can skew the high altitude ion distribution in the windward direction by dragging the ions along the magnetic field lines. These mechanisms were originally suggested by Hanson et al. 1970 and have since been treated in detailed modeling studies of the low latitude Mg^+ distributions (e.g., Hanson et al., 1972; Fesen et al., 1983; Carter and Forbes, 1999).

At middle and high latitudes (right side of Figure 15), the mechanisms for uplifting the metal ions from their source region below 100 km are basically the same as at low latitudes (i.e., **E** field and Ueast×**B** transport in regions where the magnetic field lines are inclined). When ions enter the region where their collision frequency is less than their gyrofrequency, equatorially directed atmospheric winds can further drag the ion, not across the magnetic field lines, but along the inclined magnetic field lines upward into the F-region. The upward motion is opposed by the drag of the downward diffusive flow of the major ion comprising the F-layer, O^+, so that the metal ions tend to slow and stop on the bottomside of the layer. At high polar latitudes, where large magnetospherically induced electric fields prevail, the convective flow of the ions perpendicular to B will raise the ions to even higher altitudes. The metal ions will collapse downward when they move into a region where the neutral wind and/or electric field are no longer capable of holding them up against gravity. These mechanisms were developed to explain the trends in the high latitude metal ion distributions shown in Figure 15 (papers include, Grebowsky and Brinton, 1978, Kumar et al., 1980; Grebowsky and Pharo, 1985; Bedey and Watkins, 1997). Due to the sparseness of observations, three dimensional ion distribution are not yet sufficiently known to develop high latitude models as detailed as has been done for the low latitudes, where metal ions are almost always present at high altitudes in the ionosphere.

The dynamical models for the high altitude metal ion distributions have concentrated primarily on only one of the two major metal species Mg^+ or Fe^+. However all atomic metal species that are detected in the ablation region are anticipated to be present at high altitudes. The satellite study by Kumar and Hanson (1980) identified the presence of Al^+, Na^+, Si^+ and Ca^+ and calculated their measured relative abundances from those individual mass spectra (8 second scan period) from MIMS on AE-C and AE-D in which Fe^+ exceeded 500 ions/cm^{-3}. Observed variability in the relative composition of the metal ions was very large, making the significance of mean values somewhat suspect and indicating that transport may have spatially separated the different metal ion species. For example, the Fe^+/Mg^+ ratio on AE-C was found to vary from 0.02 to 24 with an average of 1.5, and on AE-D the extremes were 0.17 to 34.2 with a mean value of 3.2. The values for Al^+/Mg^+ and Si^+/Mg^+ were approximately an order of magnitude lower.

An unresolved issue is the importance of this high altitude reservoir of long-lived atomic metal ions to the concentration and composition of the main meteor ionization layer. If the upward transport processes separate species in space, then they might have an impact on the main meteor layer composition. The high altitude metal ion content is comparable to that in the low altitude layer. Hence, if there is species separation at high altitudes, the question arises as to whether they could introduce compositional changes in the low altitude layer when they move downward. Could this play a role in the unexplained wide range of Fe^+/Mg^+ values in the main layer discussed earlier?

4. Summary

Rocket-borne ion mass spectrometric measurements discovered permanent metal ion layers in the 85 to 120 km altitude range. This is the altitude region where meteors are produced and layers of neutral metals are observed. Analysis of the relative abundance of the metals and their isotopes shows general agreement with solar system chrondritic material. The discrepancies are attributed to ion redistribution, ambiguous ion identification, and metal-atmosphere chemistry. One of the most prominent characteristics of the metal ion profiles measured in the rocket experiments is the variability in the distributions from flight-to-flight. This is due to: 1. ionosphere/atmosphere dynamics; 2. atmospheric composition changes; and/or 3. changes in the incoming distributions of the meteoroids. The first redistributes the metal ionization. (This is most evident in satellite observations of high altitude metal ions with vertical contents often comparable to those in the meteor ablation region.) The second leads to changes in chemistry of the metal ions, and the third could introduce variations in the metallic atom deposition rates or, in the case of changing mass or velocity distributions of the infalling material, lead to changes in the altitude of where the ablation occurs. Observations taken during meteor shower periods tend to show enhancements in metal ion concentrations. However, the sounding rocket studies have, thus far, not unambiguously separated metal ion distribution perturbations resulting from atmospheric and ionospheric changes from those introduced by changes in the incoming meteoroid properties.

REFERENCES

AIKIN, A. C. & R. A. GOLDBERG 1973 Metallic ions in the equatorial ionosphere, J. Geophys. Res., 78, 734-745.

AIKIN, A. C., R. A. GOLDBERG & A. AZCARRAGA 1974 Ion composition during the formation of a mid-latitude Es layer, Space Res. XIV, 283-288.

ANDERS, E. & N. GREVESSE 1989 Abundances of the elements: Meteoric and solar, *Geochimica et Cosmocimica Acta*, **53**, 197-214.

ARNOLD, F. & D. KRANKOWSKY 1977 Ion composition and electron- and ion-loss processes in the Earth's atmosphere, in *Dynamical and Chemical Coupling*, Reidel Publishing, Dordrecht, Holland, 93-127.

BEDEY, D. F. & B. J. WATKINS 1997 Large scale transport of metallic ions and the occurrence of thin ion layers in the polar ionosphere, *J. Geophys. Res.*, **102**, 9675-9681.

BENNETT, W. H. 1950 Radiofrequency mass spectrometer, *J. Appl. Phys.*, **21**, 143-147.

BRINTON, H. C., L. R. SCOTT, M.W. PHARO III, & J. T. C. COULSON 1973 The Bennett ion-mass spectrometer on Atmosphere Explorer-C and -E, *Radio Science*, **8** 323.

BROADFOOT, A. L. 1967 Twilight Ca^+ emissions from meteor trails up to 280 km, *Planet Space Sci.*, **15**, 503-513.

CARTER L. N. & J. M. FORBES 1999 Global transport and ionized layering of metallic ions in the upper atmosphere, *Ann. Geophys.*, **17**, 190-209.

CEPLECHA, Z. 1992 *Bull. Amer. Astron. Society*, **24**, 952.

CHIMONAS, G. 1969 Ion separation in temperate zone sporadic E and the layer shape, *J. Geophys. Res.*, **74**, 4189-4195.

FESEN, C. G., P. B. HAYES, & D. N. ANDERSON 1983 Theoretical modeling of low latitude Mg^+, *J. Geophys. Res.*, **88**, 3211-3223.

EARLE, G. D., T. J. KANE, R. F. PFAFF, & S. R. BOUNDS 2000 Ion layer separation and equilibrium zonal winds in midlatitude sporadic E, *Geophys. Res. Letts.*, **27**, 461-464.

FAHEY, F. E., F. C. FEHSENFELD, E. E. FERGUSON, & L. H. VIEHLAND 1981 Reactions of Si^+ with H_2) and O_2 and SiO^+ with H_2 and D_2, *J. Chem. Phys.*, **75**, 669-674.

GOLDBERG, R. A. & A. C. AIKIN 1973 Comet Encke: Meteor metallic ion identification by mass spectrometer, *Science*, **180**, 294-296.

GOLDBERG, R. A. & L. J. BLUMLE 1970 Positive ion composition from a rocket-borne mass spectrometer, *J. Geophys. Res.*, **75**, 133-142.

GOLDBERG, R. A. & G. WITT 1977 Ion composition in a noctilucent cloud region, *J. Geophys. Res.*, *82*, 2619-2627.

GREBOWSKY, J. M. & H. C. BRINTON 1978 Fe^+ ions in the high latitude F-region, *Geophys. Res. Lett.*, **5**, 791-794.

GREBOWSKY, J. M. & M. W. PHARO III 1985 The source of midlatitude metallic ions at F-region altitudes, *Planet. Space Sci.*, **33**, 807-815.

GREBOWSKY J. M. & W. D. PESNELL 1999 Meteor Showers: Modeled And Measured Effects In The Atmosphere, *American Inst. Aeronautics. & Astronautics* publication, paper no. 99-0503.

GREBOWSKY J. M., W. D. PESNELL, & R. A. GOLDBERG 1998 Do meteor showers significantly perturb the ionosphere?, *J. Atmos. Solar-Terr. Phys.*, **60**, 607-625.

HANSON, W. B. & S. SANATANI 1970 Meteoric Ions above the F2 peak, *J. Geophys. Res.*, **75**, 5503-5509.

HANSON, W. B., D. L. STERLING, & R. F. WOODMAN 1972 Source and identification of heavy ions in the equatorial F layer, *J. Geophys. Res.*, 77, 5530-5541.

HERRMANN, U., P. EBERHARDT, M. A. HIDALGO, E. KOPP, & L. G. SMITH 1978 Metal ions and isotopes in sporadic E-layers during the Perseid meteor shower, *Space Res.*, ***XVIII***, 249-252.

HOFFMAN, J. H., W. B. HANSON, C. R. LIPPINCOTT, AND E. F. FERGUSON, 1973, The retarding-potential analyzer on Atmosphere Explorer, *Radio Science*, **8**, 315.

ISTOMIN, V. G. 1963 Ions of extra-terrestrial origin in the Earth atmosphere, *Space Res*, **3**, 209-220.

JOHANNESSEN, A. & D. KRANKOWSKY 1974 Daytime positive ion composition measurement in the altitude range 73-137 km above Sardinia, *J. Atmos. Terr. Phys.*, **36**, 1233-1247.

JOHNSON, C. Y., J. P. HEPPNER, J. C. Holmes, and E. B. Meadows 1958 *Ann. Geophys.*, **14**, 475-482.

KOPP, E. 1997 On the abundance of metal ions in the lower ionosphere, *J. Geophys. Res.*, ***102***, 9667-9674.

KOPP, E., P. EBERHARDT, U. HERRMANN, & L. G. BJORN 1985 Positive ion composition of the high-latitude summer D region with noctilucent clouds, *J. Geophys. Res.*, **90**, 13,041-13,053.

KRANKOWSKY, D., F. ARNOLD, H. WIEDER, & J. KISSEL 1972 The elemental and isotopic abundance of metallic ions in the lower E-region as measured by a cryogenically pumped quadrupole mass spectrometer, *Int. J. Mass Spect. Ion Phys.*, ***8***, 379-390.

KUMAR,S. & W. B. HANSON 1980 The morphology of metal ions in the upper atmosphere, *J. Geophys. Res.*, **85**, 6783-6801.

MCNEIL, W. J. 1999 Problems in the prediction of meteor shower effects on the atmosphere, *American Inst. Aeronautics & Astronautics* publication, paper no. 99-0506.

MCNEIL, W. J., R. A. DRESSLER & E. MURAD 2001 The impact of a major meteor storm on the Earth's ionosphere: A modeling study, submitted, *J. Geophys. Res.*.

MCNEIL, W. J., S. T. LAI, & E. MURAD 1996 A model for meteoric magnesium in the ionosphere, *J. Geophys. Res.*, **101**, 5251-5259.

MCNEIL, W. J., S. T. LAI, & E. MURAD 1998 Differential ablation of cosmic dust and implications for the relative abundances of atmospheric metals, *J. Geophys. Res.*, **103**, 10,899-10,911.

NARCISI, R. S., Composition studies of the lower ionosphere, in *Physics of the Upper Atmosphere*, F. Verniani, (ed.), Editrice Compositore, Bologna, 11-59, 1971.

NARCISI, R. S. & A. D. BAILEY 1965 Mass spectrometric measurements of positive ions at altitudes from 64 to 112 kilometers, *J. Geophys. Res.*, **70**, 3687-3700.

NICOLET, M. 1955 Meteor ionization in the night-time E-layer, in "Meteors", A symposium on meteor physics: special supplement Vol. 2 to *J. Atmos. Terr. Phys.*, 99-110.

PHILBRICK, C. R., R. S. NARCISSI, R. E. GOOD, H. S. HOFFMAN, T. J. KENESHEA, M. A. MCLEOD, S. P. ZIMMERMAN & B. W. REINISCH 1973 The Alladdin Experiment - Part II, composition, *Space Res.*, **VII**, 441-449.

PLANE, J. M. C. 1991 The chemistry of meteoric metals in the Earth's upper atmosphere, *Int. Rev. Phys. Chem.*, **10**, 55-106.

PLANE, J. M. C., R. M. COX & R. J. ROLLASTAR 1999 Metallic layers in the mesopause and lower thermosphere region, *Adv. Space Res.*, **24** (11), 1559-1570.

STEINWEG, A., D. KRANKOWSKY, P. LAMMERZAHL, & B. ANWEILER 1992 Metal ions in the auroral lower E-region measured by mass spectrometers, *J. Atmos. Terr. Phys.*, *54*, 703-714.

SWIDER, W. 1969 Processes for meteoric elements in the E-region, Planet. Space Sci., 17, 1233-1246.

SWIDER, W. 1984 Ionic and neutral concentrations of Mg and Fe near 92 km, *Planet. Space Sci.*, **32**, 307-312.

VON ZAHN, U., R. A. GOLDBERG, J. STEGMAN, & G. WITT 1989 Double peaked sodium layers at high latitudes, *Planet. Space Sci., 37*, 657-667.

WHITEHEAD, J. D., 1961 The formation of the sporadic E-layer in the temperate zones, *J. Atmos. Terr. Phys.*, **20**, 49-58.

ZBINDEN, P. A., M. A. HILDAGO, P. EBERHARDT & J. GEISS, 1975 Mass spectrometer measurements of the positive ion composition in the D- and E-regions of the ionosphere, *Planet. Space. Sci.*, **23**, 1621-1642, 1975.

Table 1 Meteoric Ion Composition Relative To Cosmic Abundances

Ave. Mass amu	Element	Cosmic Abundance Anders and Grevesse [1989][1]	Goldberg and Aikin [1973][2]	Kopp [1997][3]	Krankowsky et al. [1972][4]	Zbinden et al., [1975][5]	Zbinden et al., [1975][6]
23	Na	0.053	4.6	0.98	2.8	2.2	5.0
24	Mg	1.0	1.0	1.0	1.0	1.0	1.0
27	Al	0.078		1.0	0.80	0.46	0.24
28	Si	0.93	2.2		0.00	0.0021	4.2
39	K	0.0035	4.7	0.991	2.04	3.1	1.7
40	Ca	0.056	1.3	1.01	0.64	0.81	0.42
45	Sc	0.000031	640				600
48	Ti	0.0022				0.31	
52	Cr	0.012	5.5		0.61	1.3	2.1
56	Fe	0.83	3.6	0.99	0.72	1.6	1.1
59	Co	0.0021			1.95	0.76	
60	Ni	0.046	1.9	1.04	0.80	0.80	0.56
66	Zn	0.0012				0.94	

1. Abundances are total for a given element and normalized to total abundance of magnesium.
2. Composition within a sporadic E-layer during the period of meteor shower associated with comet Enke.
3. Metal ion column densities based on five rocket flights.
4. Ten days after maximum of the Leonid meteor shower. Measurements within an ion layer at 95 km.
5. Sampling for ion layer at 95 km.
6. Sampling for ion layer at 120 km

Table 2 Isotopic Abundances of Meteoric Ions

AMU	Element	Cosmic abundance[1]	Krankowsky et al. (1997)[1]	Steinweg et al. (1992)[2] Flight F2	Steinwerg et al. (1992)[2] Flight F3	Steinweg et al. (1992)[2] Flight F4
23	Na	0.05	0.15			
24	Mg	0.79	0.82	0.74		0.76
25	Mg	0.10	0.090	0.12		0.11
26	Mg	0.11	0.091	0.14		0.13
27	Al	0.078	0.063			
39	K	0.0033	0.0063			
40	Ca	0.055	0.034			
42	Ca	0.00037	0.0011			
44	Ca	0.0012	0.0011			
52	Cr	0.048	0.0077			
54	Fe	0.049	0.049	0.053	0.055	0.049
56	Fe	0.77	0.53	0.76	0.78	0.76
57	Fe	0.023	0.028	0.026		0.026

1.Andersand Grevesse [1989]. Abundances are fraction of the total. Total abundances are normalized to total magnesium abundance.

2. Isotopic abundances are normalized to Fe^{+} abundance.

Table 3 Metal Compounds Detected in the Upper Atmosphere.

Compound	Mass amu	Ref.
K^+,NaO^+	39	(1)
Ca^+,$NaOH^+$, MgO^+	40	(1)
$MgOH^+$,$Na^+H_2O^+$	41	(1)
AlO^+	43	(2)
SiO^+	44	(2)
Sc^+, $SiOH^+$, $Al^+(H_2O)$	45	(1) (2)
SO^+	48	(1)
$CaOH^+$	57	(1)
$MgOH^+(H_2O)$	59	(1)
$Na(CO_2)^+$	67	(1)
FeO^+	72	(1) (3)
$FeOH^+$	73	(3)
$Fe^+(H_2O)$	74	(1)
$MgOH^+(H_2O)_2$	77	(1)
FeO_2^+	88	(3)
$FeO^+(H_2O)$	90	(3)
$Fe^+(H_2O)_2$	92	(3)
$FeO_2^+(H_2O)$	106	(1)
$FeO^+(H_2O)_2$	108	(3)
$Fe^+(H_2O)_3$	110	(3)
$MgOH^+(H_2O)_4$	113	(1)
$FeO_2^+(H_2O)_2$	124	(3)
$FeO^+(H_2O)_3$	126	(3)
$Fe^+(H_2O)_4$, Fe_2O^+	128	(3)
$MgOH^+(H_2O)_6$	149	(1)
$MgOH^+(H_2O)_7$	167	(1)

(1) Kopp et al. (1985); (2) Zbinden et al. (1975); (3) Goldberg and Witt (1977)

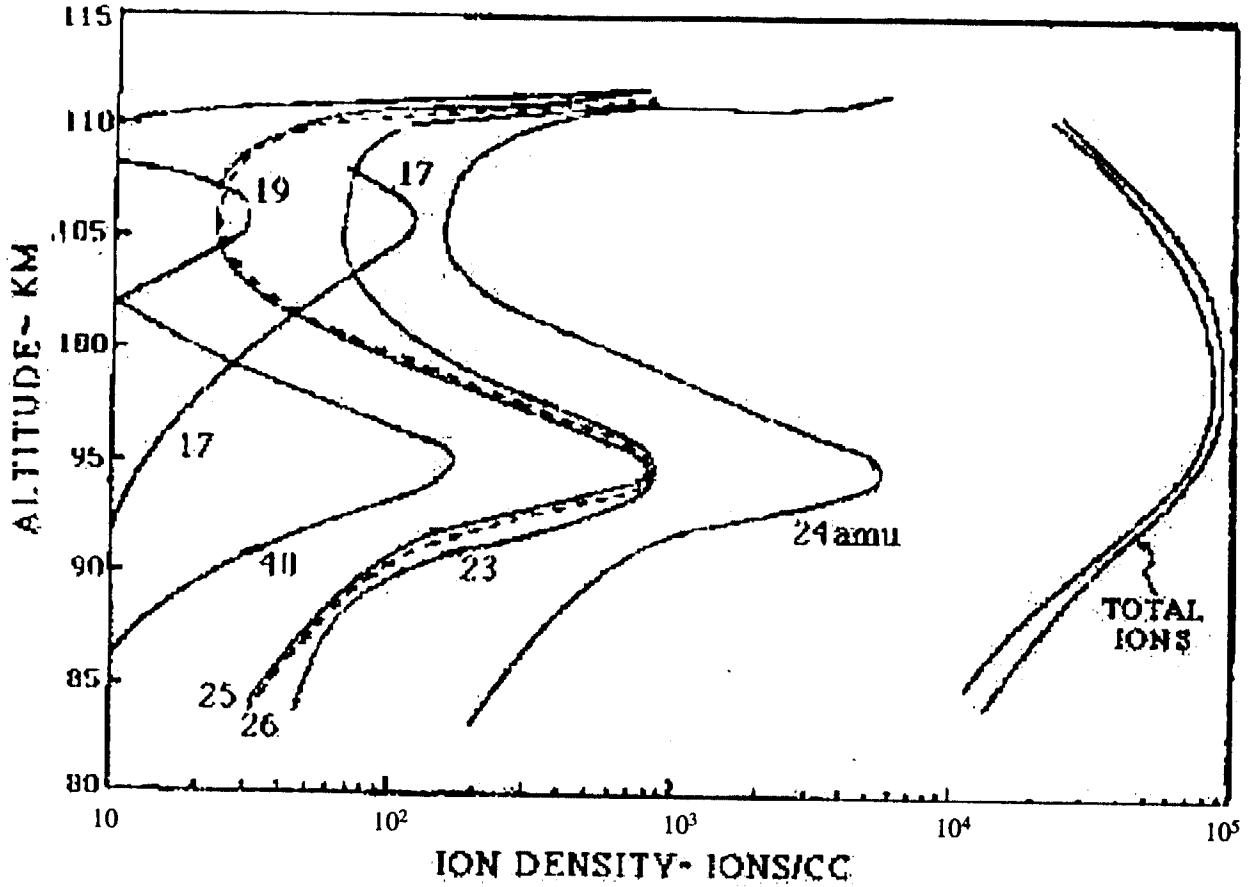

Figure 1. First complete profile of main metal ion layer (from Narcisi and Bailey, 1965). The curves are labeled by the atomic masses of the measured positive ions. Mg^+ corresponds to 23, 24 and 26 amu. Total ion densities were measured by electrostatic analyzers. A second metal ion layer was skirted at apogee.

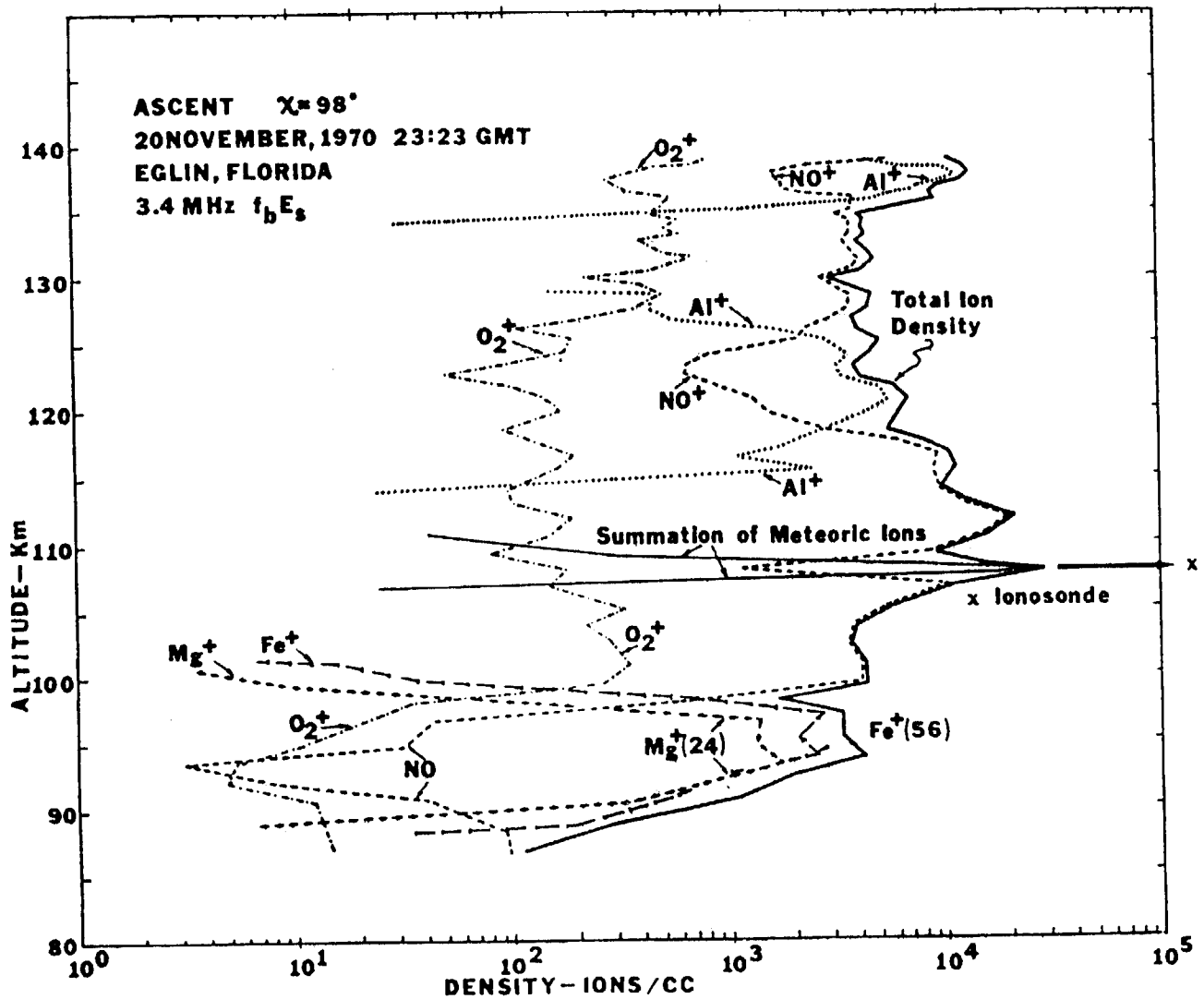

Figure 2. Midlatitude nightside measurements of positive ions (Philbrick et al., 1973). Two layers of metal ions were traversed. The major molecular ion concentrations were reduced when the metal ions peaked. The upper narrow layer was associated with blanketing sporadic E conditions measured by ground-based radio soundings. The species Al^+ was the product of a chemical release experiment.

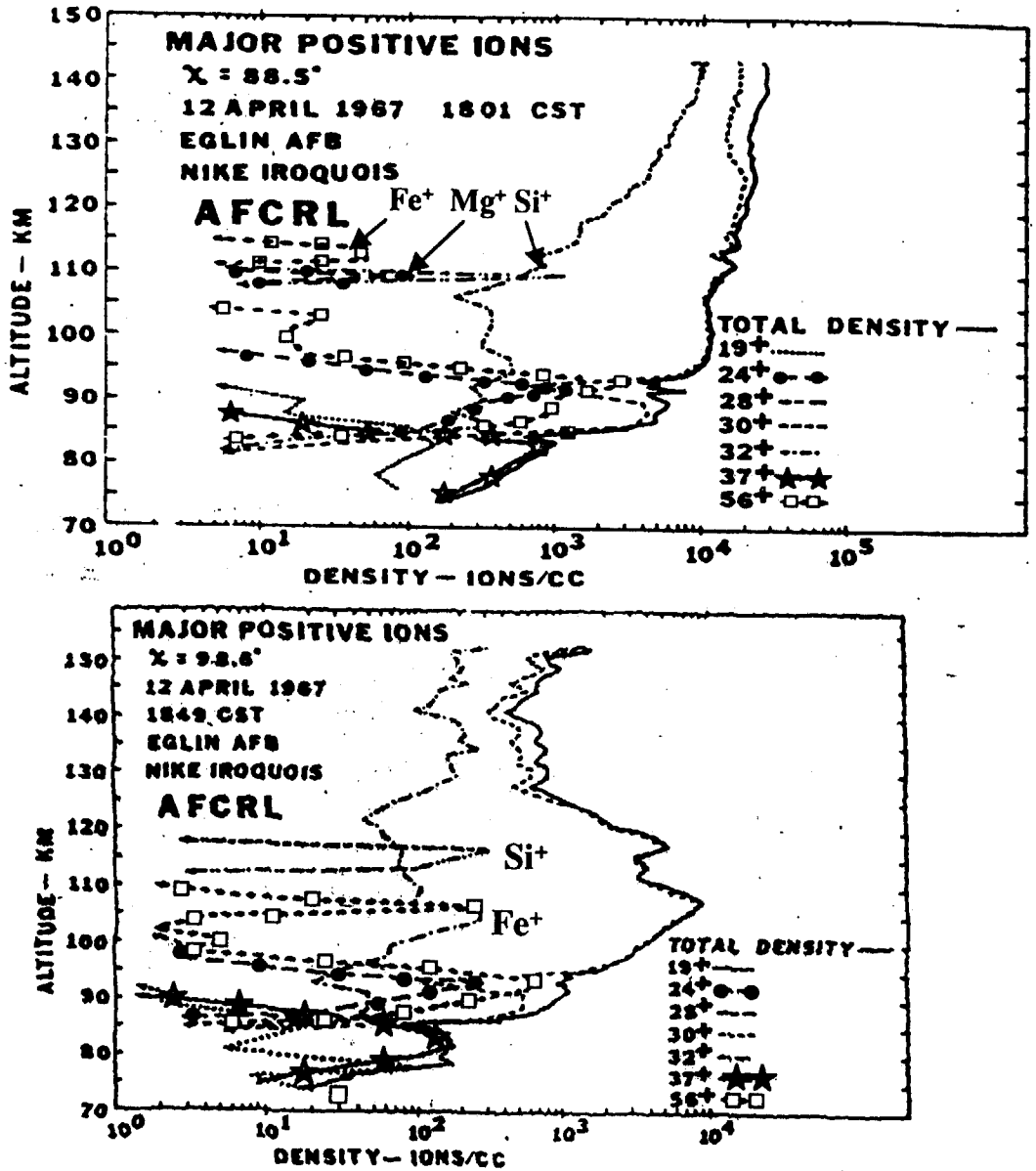

Figure 3. Measurements from 2 flights less than 1 hour apart, before (top) and after (bottom) sundown (Narcisi et al., 1971). Within this short period the metal ion layers above 100 km completely changed. The metal ions below 95 km showed a reduction in density. The two plots are positioned so that their concentration scales match each other.

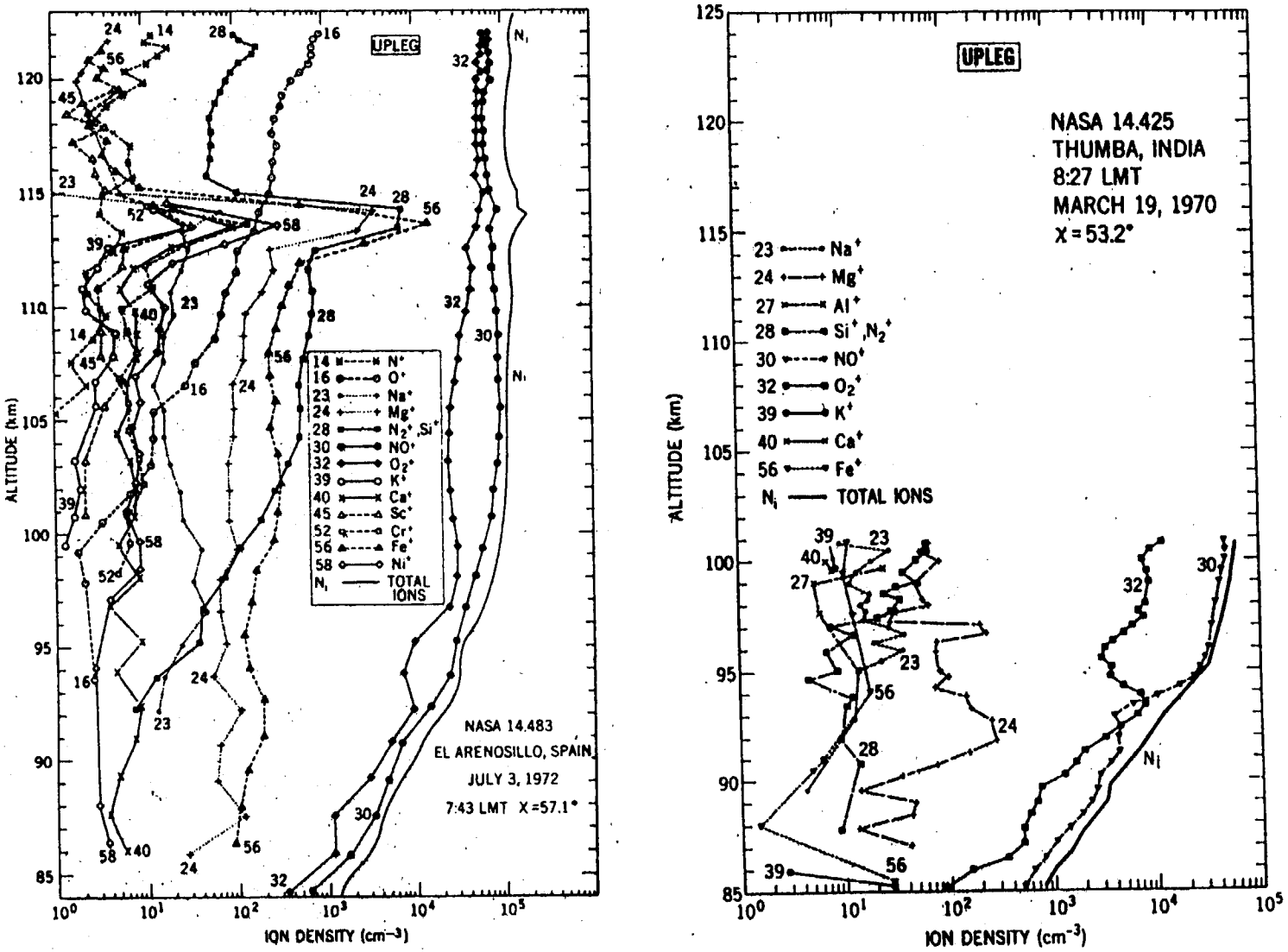

Figure 4. Examples where metal ions do not layer near 95 km. On left, a middle latitude measurement (Goldberg and Aikin, 1973; Aikin et al., 1974), only the layer near 114 km is prominent. On right, a low latitude measurement (Aikin and Goldberg, 1973), the metal ion peak is structured and Fe^+ is depleted relative to Mg^+. The measurement on the left was taken during the β Taurids shower.

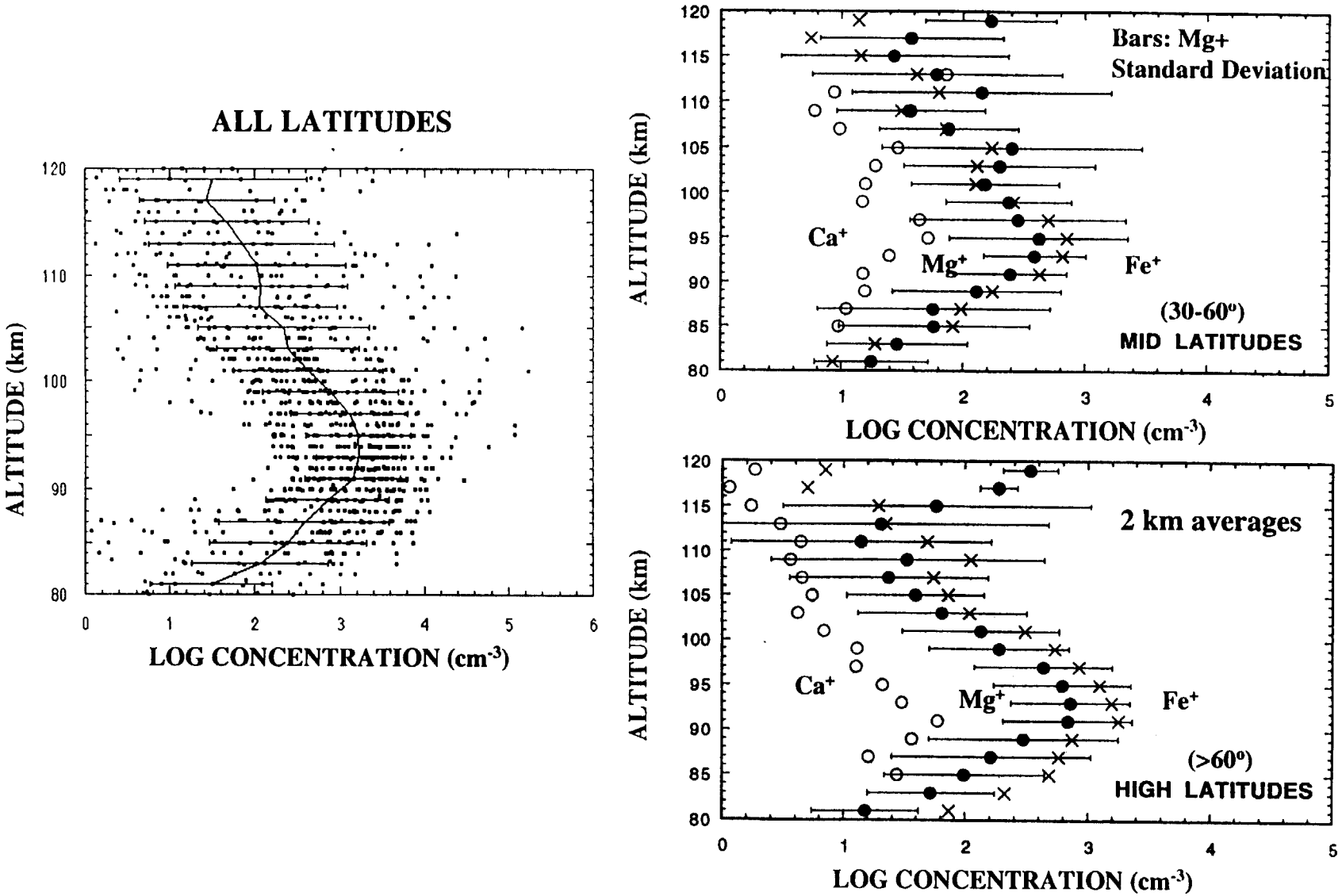

Figure 5. Left: total metal ion concentrations from all published positive ion measurements (1 km altitude interpolation). The points correspond to total metal ion densities when that was plotted in a publication otherwise it is the sum of Mg^+ and Fe^+, the two dominant metal ions. There is more than an order of magnitude scatter in the concentrations at all altitudes. Right: averages for 3 species for middle and high latitudes.

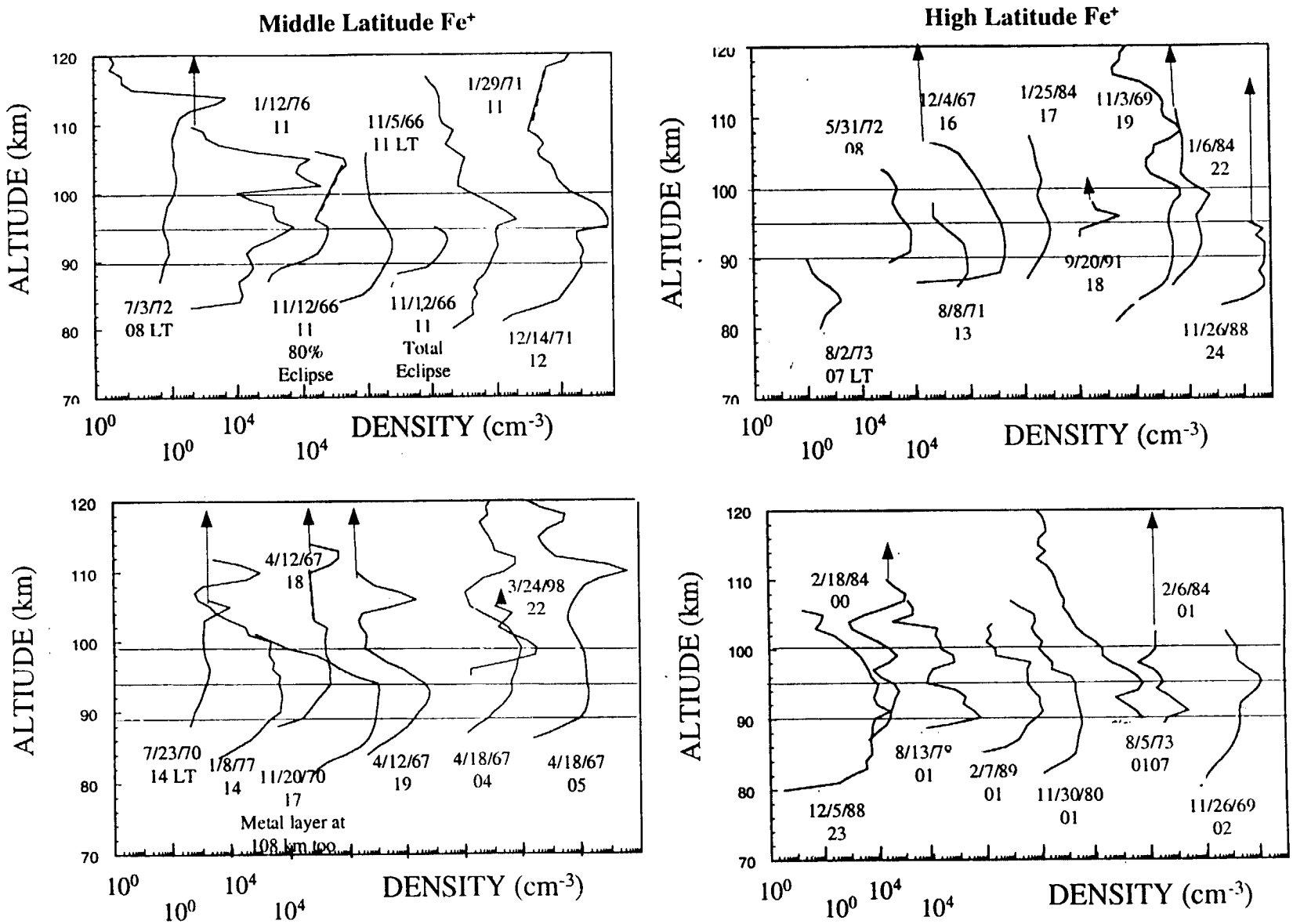

Figure 6. Altitude profiles of Fe^+. All middle latitude (between 30^O and 60^O latitude) measurements are on the left. Measurements poleward of this zone are on the right. The density scales for individual profiles are offset by a factor of 100 from each other. Data are plotted sequentially in local time. Arrows indicate altitudes where data were taken but no Fe^+ reported.

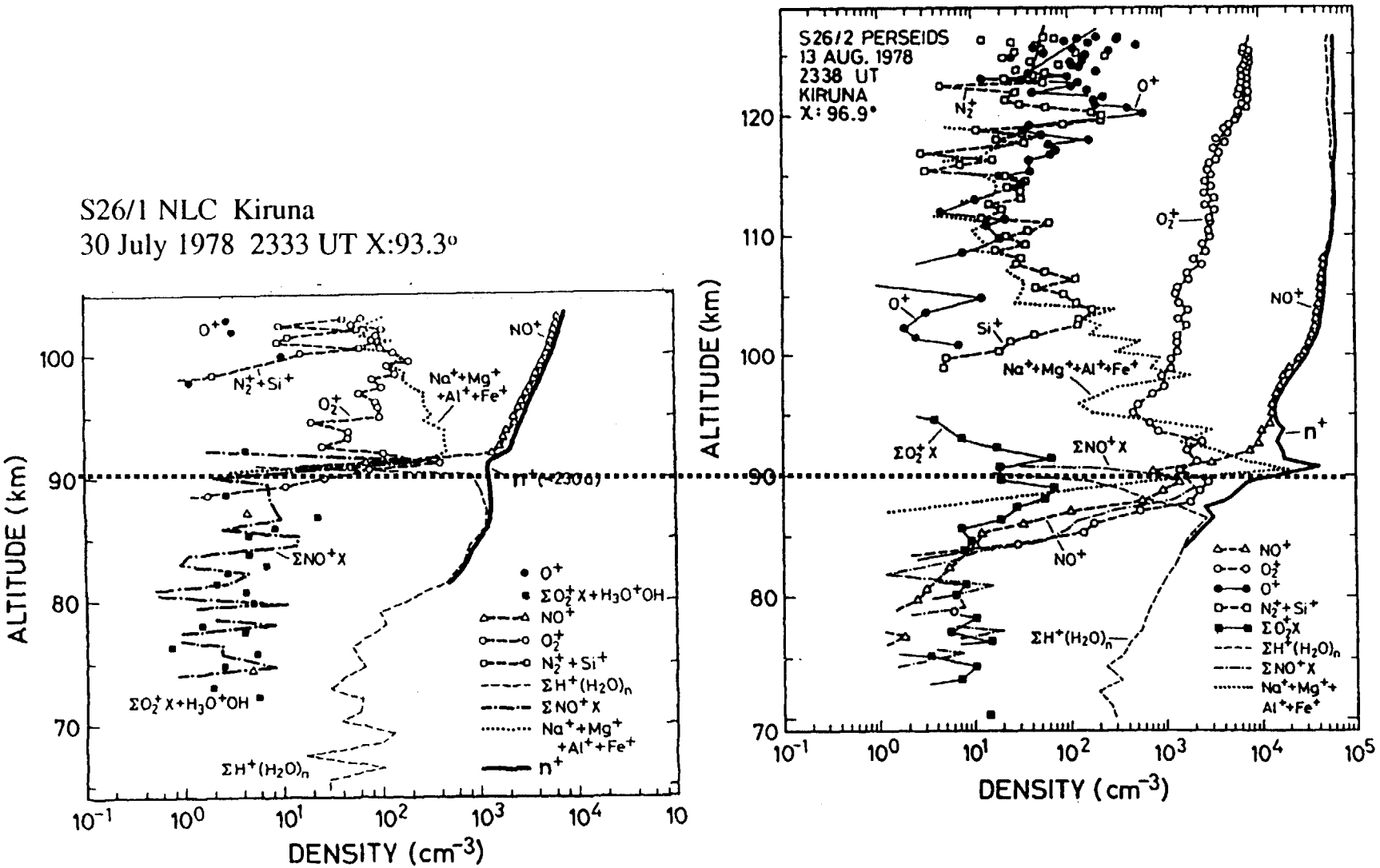

Figure 7. Two high latitude measurements through noctilucent cloud regions (Kopp et al., 1985). On the bottomsides of the metallic ion layers, the metal ion concentrations drop more than an order of magnitude in 1-2 km, where hydrates and negative aerosols (not shown here) were detected. Interactions of the metal ions with negative aerosols is responsible for the metal ion loss. The measurements were taken from the same location before and during the Perseid shower.

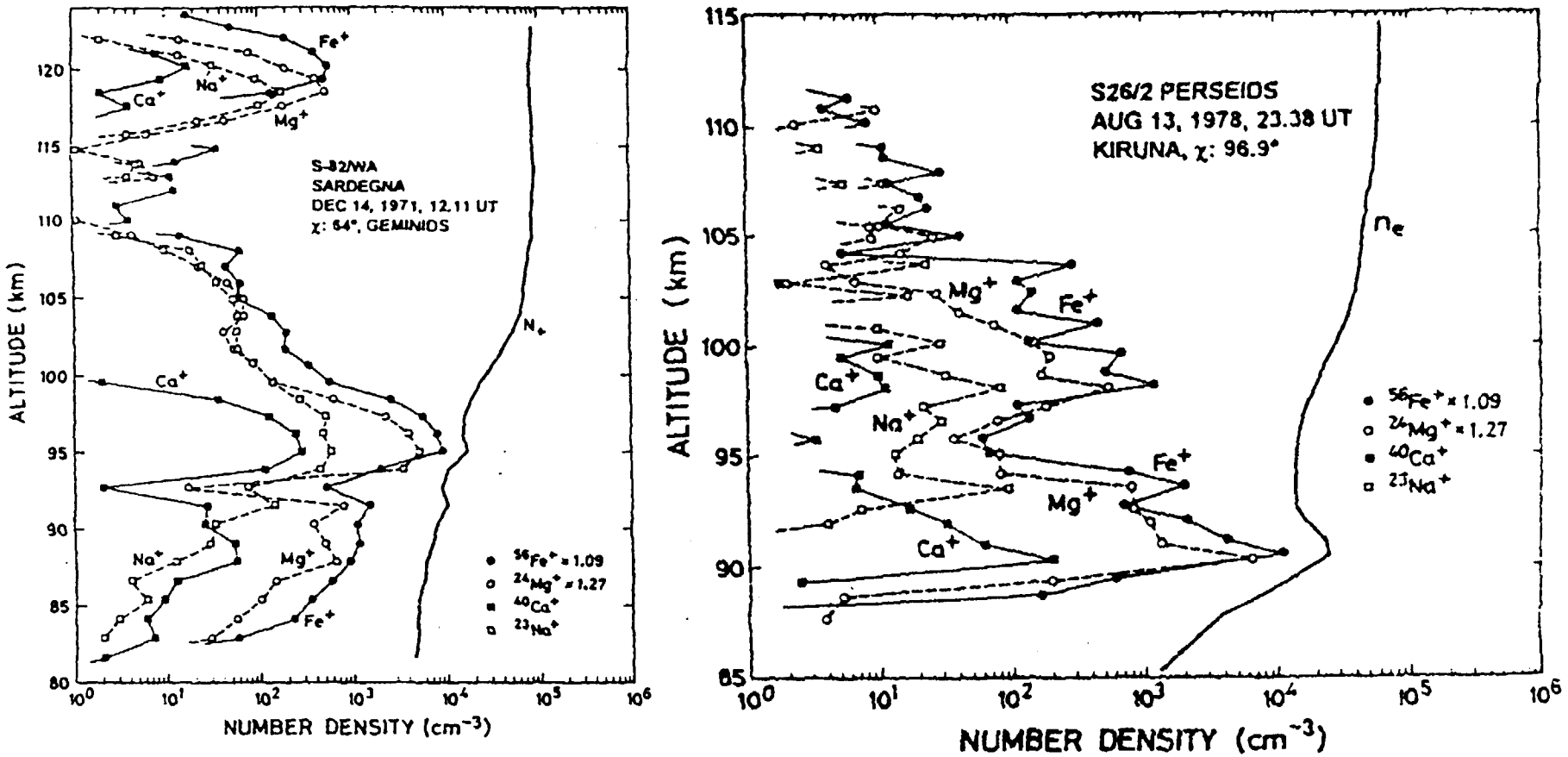

Figure 8. Two sets of ion measurements associated with meteor showers (from Kopp, 1997). Measurements on the left (at a middle latitude) were obtained during the maximum of the Geminid shower and that on the right (at a high latitude), one day following the maximum activity of the Perseid shower. The main peak metallic ion densities observed were higher than the average non-shower concentrations.

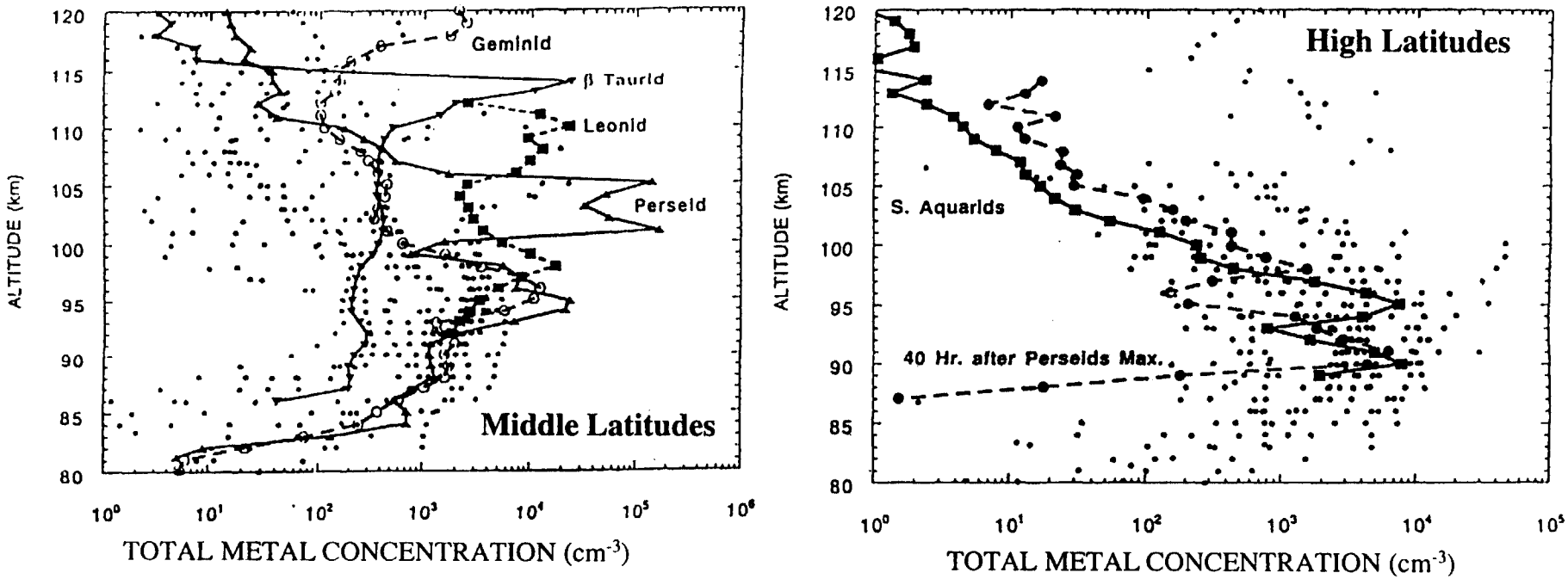

Figure 9. A comparison of individual profiles of the total metal ion density for showers superimposed on 1 km interpolated values for non-shower periods (From Grebowsky et al., 1998). Middle latitude observations (left) show that shower measurements have higher peak densities - particularly in the upper altitude layers. The high latitude observations don't show a clear trend.

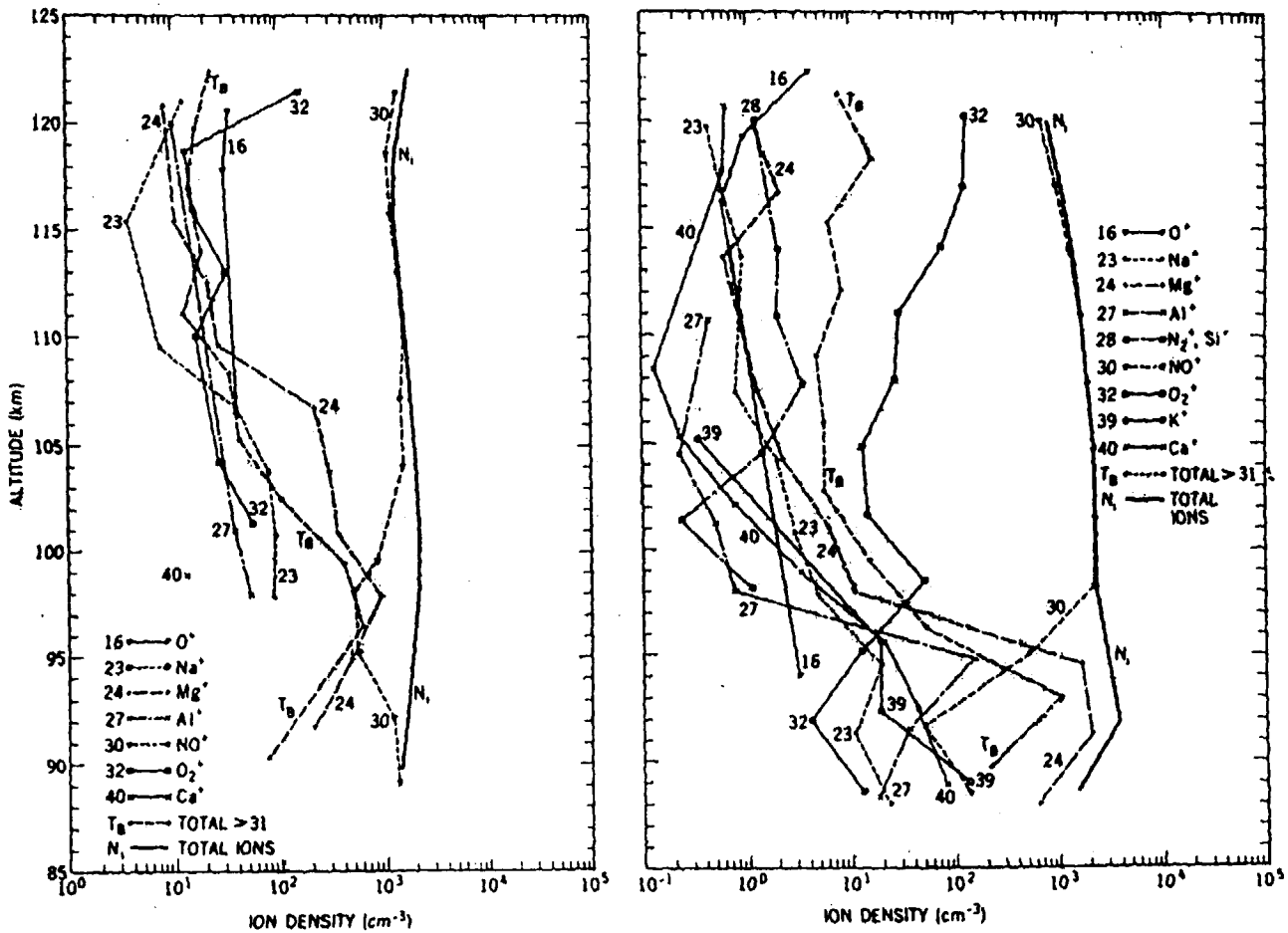

Figure 10. Upleg positive ion measurements (Aikin and Goldberg, 1973) over Thumba, India on the night of March 9-10, 1970 at 1938 MLT (left) and 0108 LMT (right). Metal layer moved downward ~7 kilometers - its displacement was consistent with magnitude of coincidently observed downward drift of higher altitude F-layer.

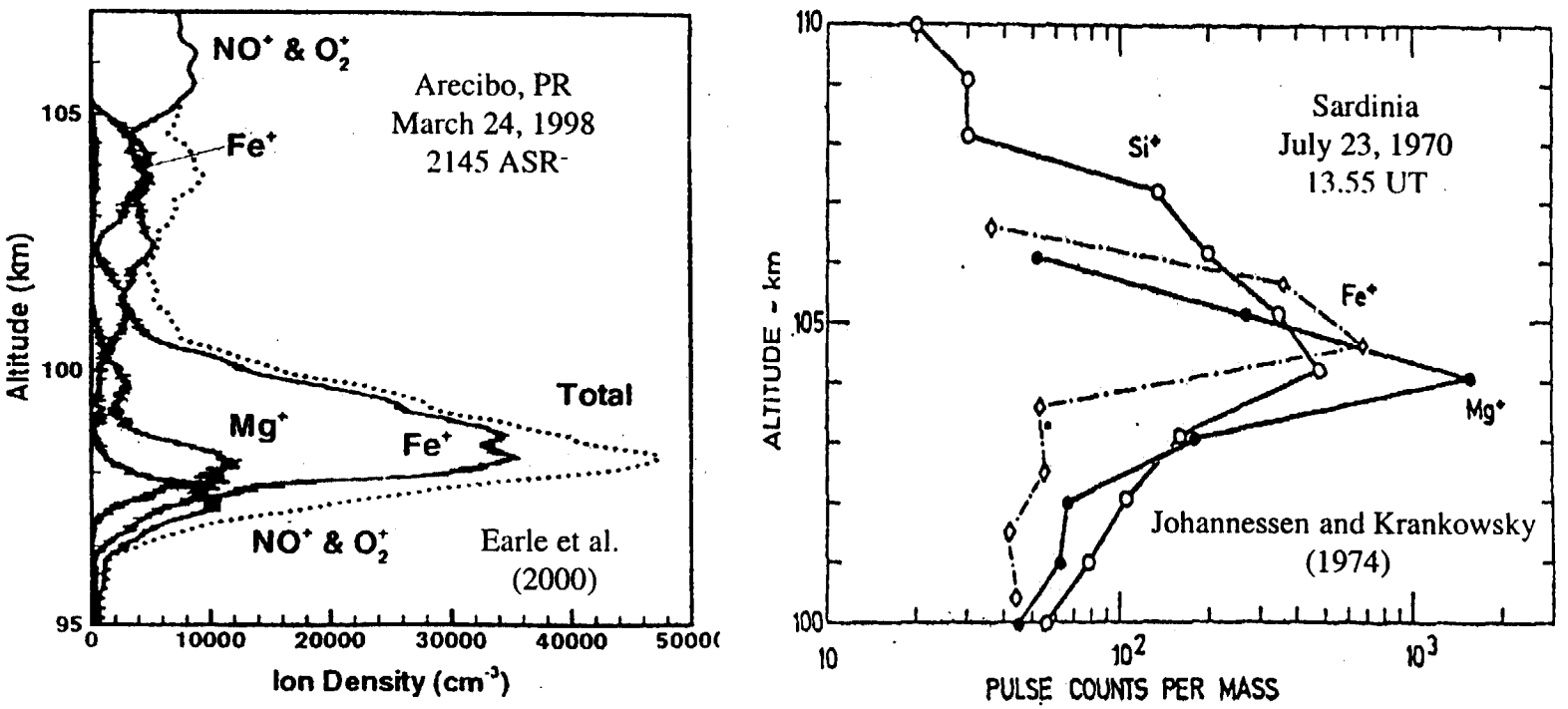

Figure 11. Two middle latitude examples of metal ion species whose layers are separated in altitude. In both examples the lighter ion, Mg^+, peaks at lower altitudes than the heavy ion Fe^+. This is what is expected for the transport of plasma to a node in the vertical shear of the horizontal wind from above and below. The data on the right is in the form of uncorrected count rates.

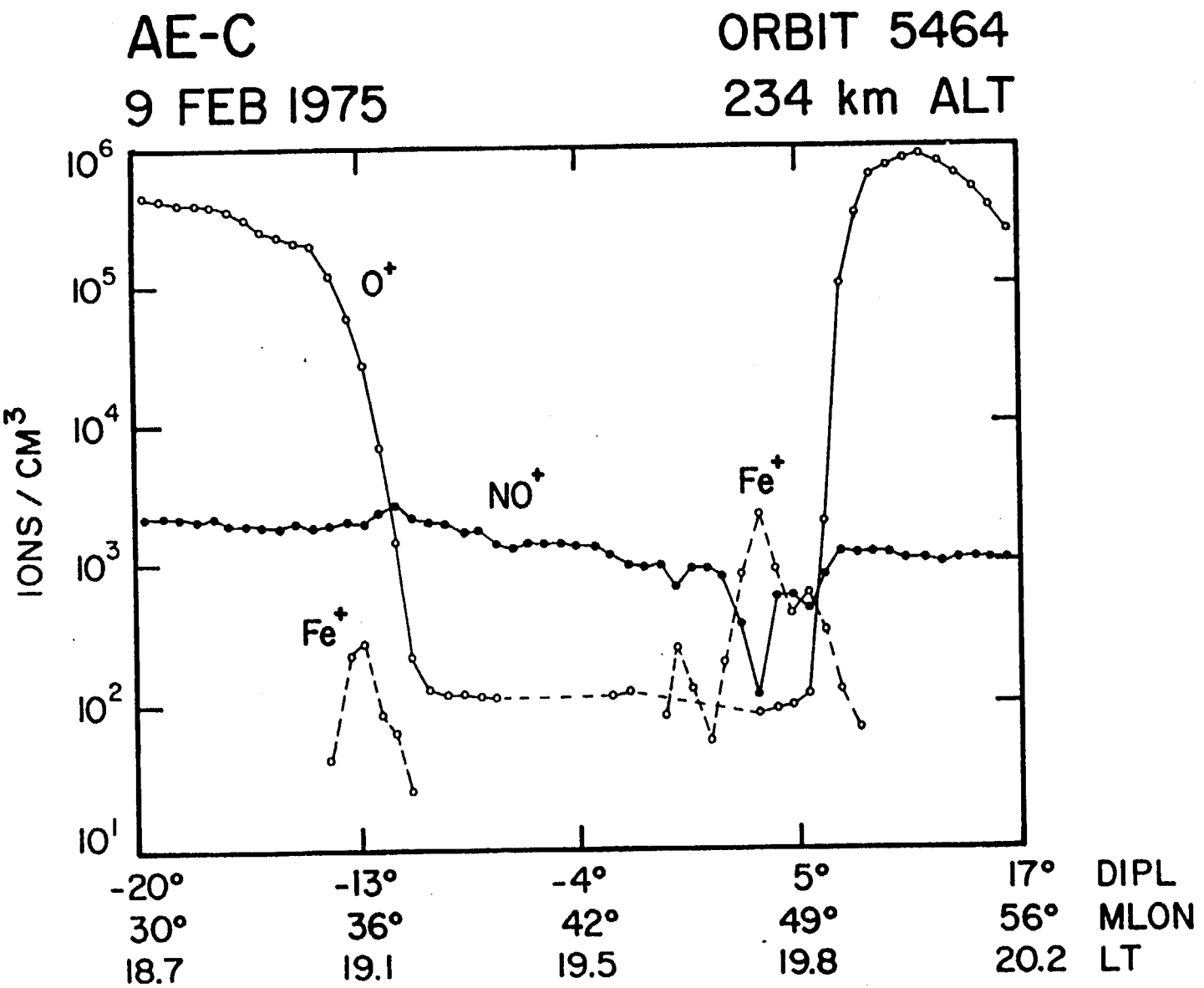

Figure 12. Low latitude measurements of major ions at 234 km by the Bennett Ion Mass Spectrometer on Atmosphere Explorer C. Even at this high altitude, the metal ion Fe+ is detected and in one region is the dominant ion.

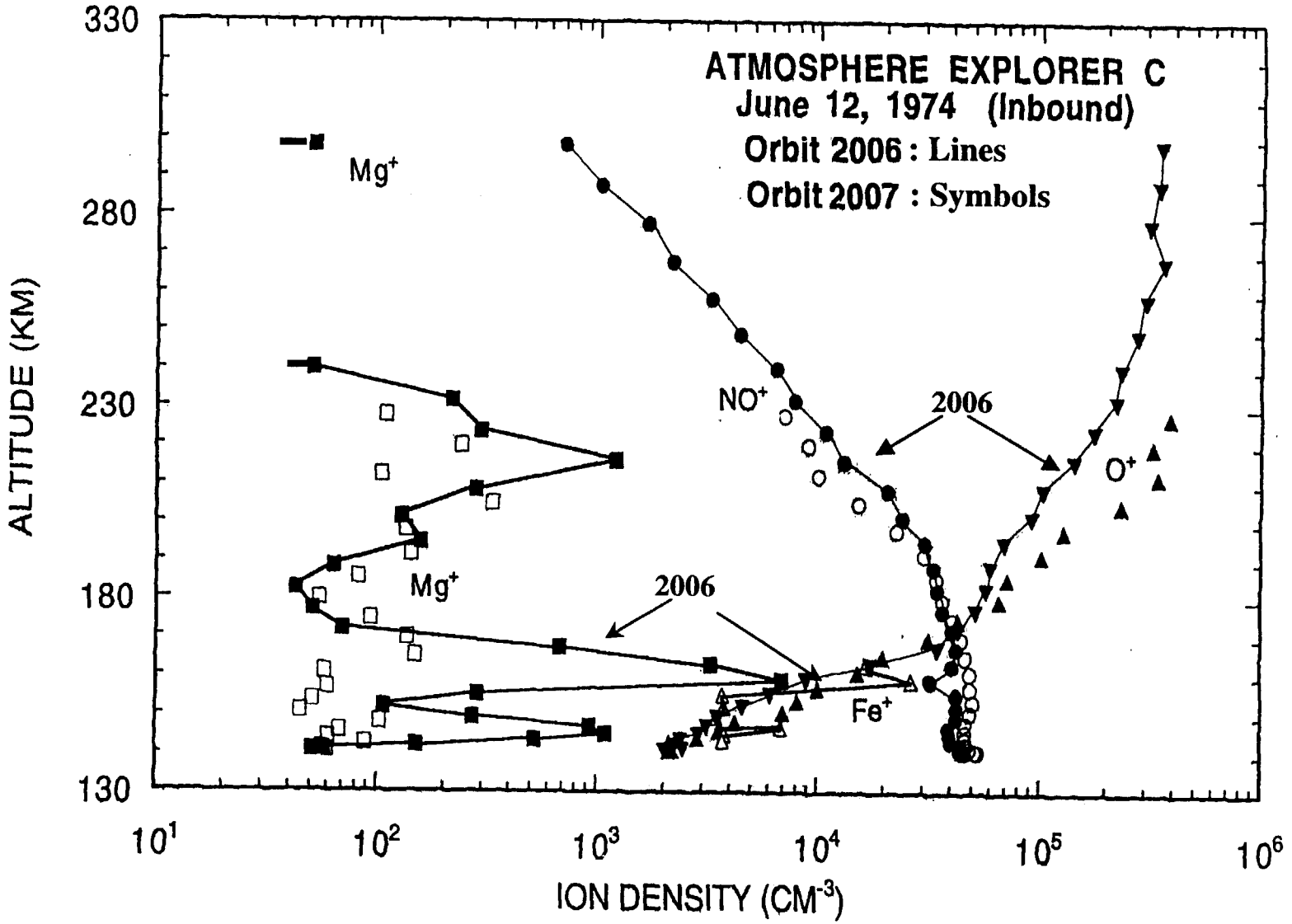

Figure 13. Measurements on two consecutive eccentric orbits of AE-C just on the dayside of dawn at middle latitudes. Mg^+ was measured by the Magnetic Ion Mass Spectrometer (MIMS). Fe^+ was detected by the Bennett Ion Mass Spectrometer (BIMS) on only orbit 2006. Metal ions were detected continuously through the bottomside of the F-layer (composed predominantly of O^+) down to perigee. Data was obtained from National Space Science Data Center-A

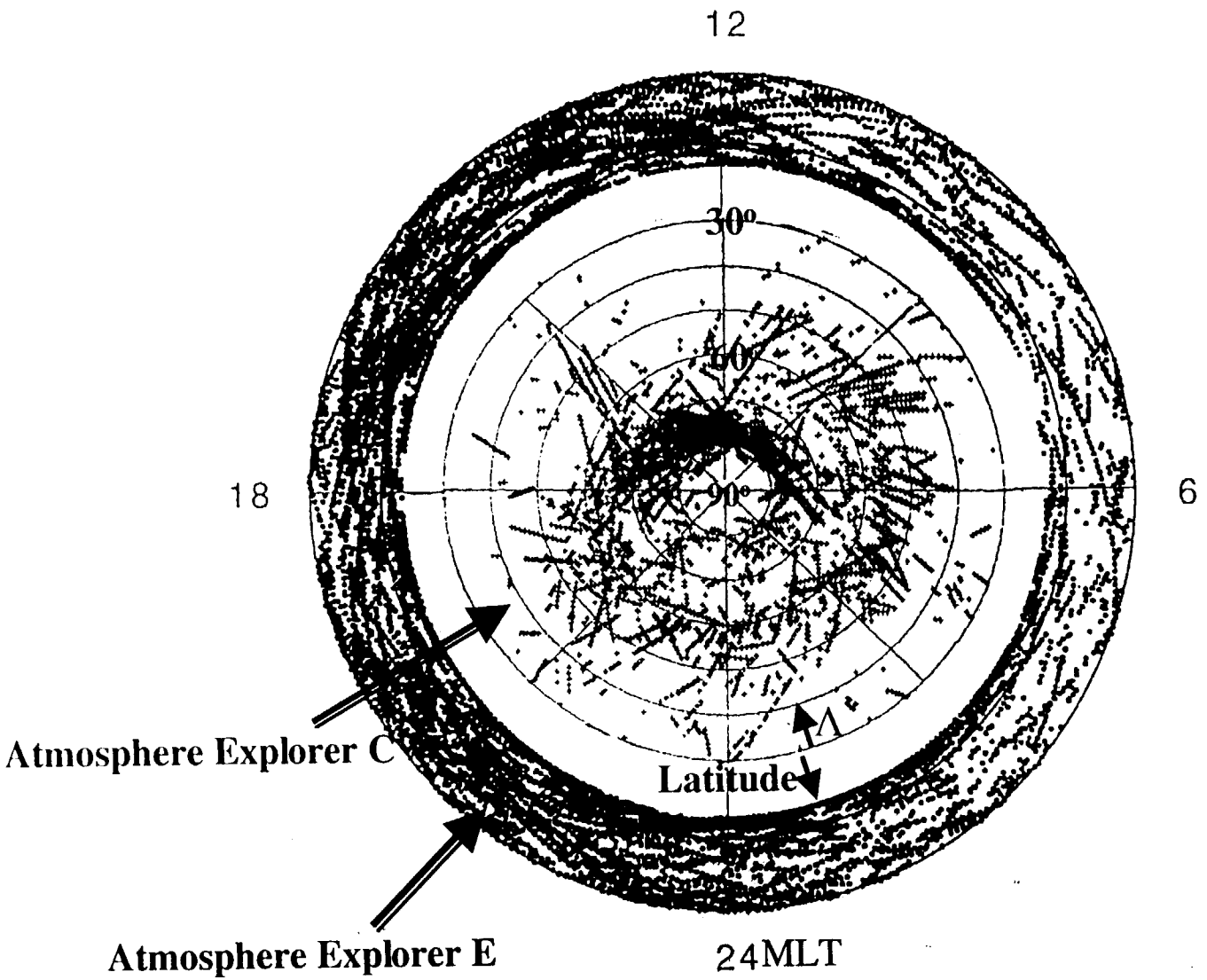

Figure 14. Measurement locations of Fe^+ ions with concentrations greater than 30 cm^{-3} from AE-C and AE-E between ~150 km and 400 km. It is a composite of AE-E low latitude data, obtained from the National Space Science Data Center-A, superimposed on published AE-C data (Grebowsky and Pharo, 1985) poleward of 30° magnetic latitude. The coordinate of magnetic latitude (Λ) is used in plot for >30°, while the absolute value of the geodetic latitude is used for lower latitudes.

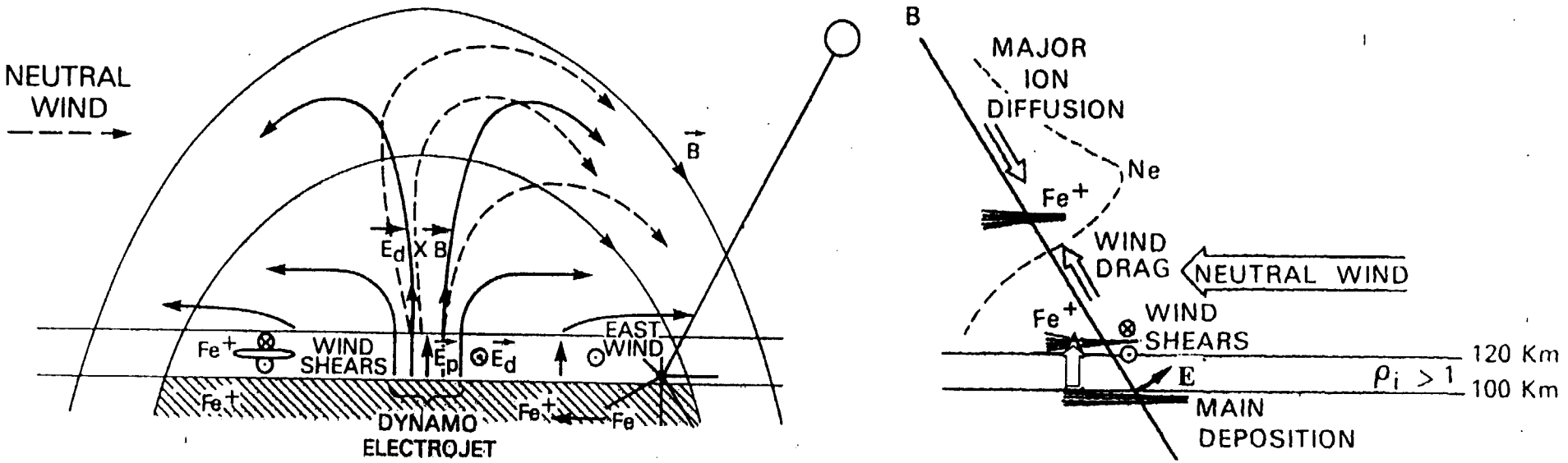

LOW LATITUDE

HIGH LATITUDE

Figure 15. Mechanisms responsible for transporting metal ions up from the meteor ablation region. At low latitudes ion vertical motions are associated with ionospheric dynamo electric fields produced by atmospheric winds dragging ions across the magnetic field. At high latitudes magnetospherically induced electric fields are important. At low altitudes, where the ratio, ρ, of the ion-neutral collision frequency to ion gyrofrequency exceeds 1, **E** fields can transport positive ions vertically across **B**. Above ~ 130 km the neutral wind drags the ions along the magnetic field lines) across magnetic field lines. Downward diffusion flows of O^+ near the F-region peak impedes the upward wind drag of the ions.